

UNIVERSIDADE TÉCNICA DO ATLÂNTICO
INSTITUTO DE ENGENHARIA E CIÊNCIAS DO MAR
WEST AFRICAN SCIENCE SERVICE CENTRE ON CLIMATE CHANGE
AND ADAPTED LAND USE

Master Thesis

**EVALUATION OF THE IMPACTS OF
REGIONAL ATMOSPHERE-OCEAN
COUPLING ON THE HISTORICAL
PRECIPITATION OVER THE CABO
VERDE ARCHIPELAGO**

ALMOUSTAPHA AMADOU MALAM LACHO

Master Research Program on Climate Change and Marine Sciences

São Vicente
2023

UNIVERSIDADE TÉCNICA DO ATLÂNTICO
INSTITUTO DE ENGENHARIA E CIÊNCIAS DO MAR
WEST AFRICAN SCIENCE SERVICE CENTRE ON CLIMATE CHANGE
AND ADAPTED LAND USE

Master Thesis

**EVALUATION OF THE IMPACTS OF
REGIONAL ATMOSPHERE-OCEAN
COUPLING ON THE HISTORICAL
PRECIPITATION OVER THE CABO
VERDE ARCHIPELAGO**

ALMOUSTAPHA AMADOU MALAM LACHO

Master Research Program on Climate Change and Marine Sciences

Supervisor | Prof. Dr. Nilton Évora do Rosário
Co-supervisor | Dr. Armelle Reça C. Remedio

São Vicente
2023

UNIVERSIDADE TÉCNICA DO ATLÂNTICO
INSTITUTO DE ENGENHARIA E CIÊNCIAS DO MAR
WEST AFRICAN SCIENCE SERVICE CENTRE ON CLIMATE CHANGE
AND ADAPTED LAND USE

**Evaluation of the impacts of regional atmosphere-ocean coupling on the historical
precipitation over the Cabo Verde archipelago**

Almoustapha Amadou Malam Lacho

Master's thesis presented to obtain the master's degree
in Climate Change and Marine Sciences, by the
Institute of Engineering and Marine Sciences, Atlantic
Technical University in the framework of the West
African Science Service Centre on Climate Change and
Adapted Land Use

Supervisor

Prof. Dr. Nilton Évora do Rosário
Federal University of Sao Paulo – Brazil

Co-supervisor

Dr. Armelle Reça C. Remedio
Climate Service Centre Germany (GERICS) - Germany

UNIVERSIDADE TÉCNICA DO ATLÂNTICO
INSTITUTO DE ENGENHARIA E CIÊNCIAS DO MAR
WEST AFRICAN SCIENCE SERVICE CENTRE ON CLIMATE CHANGE
AND ADAPTED LAND USE

**Evaluation of the impacts of regional atmosphere-ocean coupling on the historical
precipitation over the Cabo Verde archipelago**

Almoustapha Amadou Malam Lacho

Panel defense

President

Prof. Dr. Estanislau Lima

ISECMAR-UTA

Examiner 1

Prof. Dr. William David Cabos Navares

University of Alcalá, Madrid-Espanha

Examiner 2

Dr. Issaharou Matchi Issiaka

University of Diffa, Niger

Examiner 3

Dr. Sandro Veiga

Nanjing university, China

Publication list

Almoustapha Amadou, M. L., Évora do Rosário, N., Remedio, A. R., Weber, T., Cabos, W., & Sein, D. V. (2023, September 25-30). Impacts of ocean-atmosphere coupling on precipitation in small islands: a case study of the Cabo Verde archipelago. [Poster presentation]. Presented at the International Conference on Regional Climate-CORDEX 2023 (ICRC-CORDEX 2023) in Trieste, Italy.



Financial support

The German Federal Ministry of Education and Research (BMBF) in the framework of the West African Science Service Centre on Climate Change and Adapted Land Use (WASCAL) through WASCAL Graduate Studies Program in Climate Change and Marine Sciences at the Institute for Engineering and Marine Sciences, Atlantic Technical University, Cabo Verde.

Dedication

I wish to strongly and passionately dedicate this work to my mother Habsou Mahaman and to my late father Amadou Malam Lacho whom I cherish so much and who have labored to give me a solid foundational upbringing that was enhanced and further sharpened by my teachers to make my humble self. I also dedicate it to my brothers and sisters. In addition, all those who support me from near or far, especially my uncle Buhari Mahaman and Moussa Soulé, PhD.

You have always been my model, my inspiration. Your support, your encouragement, and your prayers have always accompanied me.

This work expresses my gratitude and affection.

Acknowledgements

I would start by thanking the almighty God for His unconditional blessings and who voluntarily allowed me to get to this position today,

I would like to express my gratitude to Prof. Dr Nilton Évora do Rosario and Dr. Armelle Reça C. Remedio, who have accompanied me throughout this learning process. I thank them for their support, guidance, motivation and patience. They proved that " with some motivation and the right people around one can achieve significant and many things ". Working with them always motivated me to work hard, be diligent and do better.

I am equally thankful to the Director of WASCAL Cabo Verde, Dr. Corrine Almeida, the Deputy Director, Dr António Pinto Almeida, the Scientific coordinator Dr. Estanislau Baptista Lima and the staff for all their support and constructive criticism during different stages of my studies.

I would not complete this without an acknowledgement to the Federal Ministry of Education and Research (BMBF) that funded the West Africa Science Service Center on Climate Change and Adapted Land Use (WASCAL) which offered me the Master Research Program in Climate change and Marine Sciences fellowship.

I would like to express my gratitude to Climate Service Center Germany (GERICS) for accepting to host my visit to their office, especially Dmitry V. Sein and William Cabos who supported me during my stay.

Thanks to all my colleagues of the 3rd cohort, my family and friends for their encouragement, support and prayers during this process.

And finally, my heartfelt gratitude to all the staff of the Institute of Engineering and Marine Sciences (ISECMAR) of the Atlantic Technical University and more so to all my lecturers for all forms of guidance they offered during my studies period.

Resumo

Informações climáticas precisas com a resolução espacial e temporal adequada são cruciais para a prestação de serviços climáticos adaptados para os pequenos estados insulares. O downscaling dinâmico dos modelos climáticos globais é normalmente utilizado para produzir dados sobre as alterações climáticas regionais. No entanto, as deficiências na integração das interações atmosfera-oceano podem constituir uma importante fonte de distorção da precipitação do modelo, especialmente no caso de pequenas ilhas em regiões tropicais. Neste estudo, avaliamos o impacto de um modelo regional de acoplamento atmosfera-oceano na simulação da precipitação no arquipélago de Cabo Verde. Comparamos as simulações de um modelo acoplado (ROM) e de um modelo não acoplado (REMO) numa resolução espacial de $0,22^\circ \times 0,22^\circ$. Os modelos foram conduzidos com a reanálise ERA-INTERIM. Para avaliar os seus resultados, os dados CHIRPS foram utilizados como referência observacional. As análises centraram-se na capacidade de simular os padrões sazonais e espaciais da precipitação, que foram avaliados utilizando a métrica do Valor Acrescentado (AV). Também examinámos os modelos para reproduzir as anomalias de precipitação anual e as secas a longo prazo. Os resultados mostraram que ambos os modelos podem simular adequadamente o ciclo sazonal da precipitação e a heterogeneidade espacial da precipitação entre as sub-regiões. Contudo, durante a estação das chuvas (ASO), o ROM tem um melhor desempenho na simulação das quantidades de precipitação, especialmente durante o pico da estação (setembro), quando o REMO sobrestima a precipitação. Consequentemente, foi registada uma AV positiva em todas as ilhas durante a estação das chuvas. No que respeita à variabilidade interanual das anomalias, o acoplamento teve um melhor desempenho em todo o país e nas ilhas do sul, e os modelos não tiveram um bom desempenho nas ilhas do norte e do leste. Para a seca a longo prazo, de alguma forma ambos os modelos conseguiram simular consistentemente a alternância de condições secas e húmidas entre os anos 1980 e 1990 para Cabo Verde e as ilhas do sul. No entanto, posteriormente, faltou-lhes consistência entre eles e em relação à observação. Estes resultados sugerem os benefícios da utilização de um modelo acoplado atmosfera-oceano para simular a precipitação sobre o arquipélago de Cabo Verde, particularmente sobre as ilhas do Sul.

Palavras-chave: Modelagem climática regional; Acoplamento Oceano-atmosfera, Alterações Climáticas Regionais; Pequenas ilhas; África Ocidental; Cabo Verde.

Abstract

Accurate climate information at the appropriate spatial and temporal resolution is crucial for developing and providing tailored climate services for small islands. Dynamical downscaling of global climate models is commonly used to produce regional climate change data. However, deficiencies in the integration of atmosphere-ocean interactions can be an important source of bias to the model's precipitation, especially for small islands in tropical regions. In this study, we evaluate the impact of a regional atmosphere-ocean coupling model on the simulation of precipitation over Cabo Verde archipelago. We compare simulations from a coupled model (ROM) and an uncoupled model (REMO) at a spatial resolution of $0.22^\circ \times 0.22^\circ$. Models were driven with the ERA-INTERIM reanalysis. To evaluate their results the CHIRPS data was used as the observational reference. The analyses were focused on the ability to simulate the seasonal and spatial patterns of rainfall, which were assessed using the Added Value (AV) metric. We also examined the models for reproducing annual precipitation anomalies and long-term droughts. The results showed that both models can adequately simulate the seasonal cycle of precipitation and the spatial heterogeneity of rainfall among the sub-regions. However, during the rainy season (ASO), ROM performs better in simulating precipitation amounts, especially during the peak of the season (September) when REMO overestimate rainfall. As a consequence, positive AV was found over all islands during the rainy season. For the interannual variability of anomalies, coupled performed better for the entire country and the southern islands, and models did not perform well for the northern and eastern islands. For the long-term drought, somehow both models managed to simulate consistently the alternation of dry and wet conditions between the 1980's and 1990's for Cabo Verde and the southern islands. Still, afterward, they lacked consistency among them and against observation. These results suggest the benefits of using a coupled atmosphere-ocean model to simulate precipitation over the Cabo Verde archipelago, particularly over the Southern Islands.

Keywords: Regional climate modelling; Atmosphere–ocean coupling, regional climate change; Small islands; West Africa; Cabo Verde.

Abbreviations and acronyms

AEJ	African easterly jet
AOGCM	Atmosphere Ocean Global Circulation Model
ASO	August, September, and October
AV	Added Value
CHIRPS	Climate Hazards Group InfraRed Precipitation with Station data
CORDEX	Coordinated Regional Downscaling Experiment
EASM	East Asian summer monsoon
EROS	Earth Resources Observation and Science
EWs	Easterly Waves
GCMs	Global Climate Models
GERICS	Climate Service Center Germany
INMG	National Meteorological institute
IPCC	Intergovernmental Panel on Climate Change
ITCZ	Intertropical Convergence Zone
MPI-ESM-LR	Max Planck Institute Earth System Model - Low Resolution
MPIOM	Max Planck Institute Ocean Model
RCD	Regional Climate Downscaling
RCMs	Regional Climate Models
REMO	Regional atmospheric Model
ROM	Regionally-coupled model
SAL	Saharan Air Layer
SHL	Saharan Heat Low
SIDS	Small Island Development State
SPEI	Standardized Precipitation Evapotranspiration Index
SPI	Standardized Precipitation Index

SST	Sea Surface Temperature
UNFPA	United Nation Population Fund
WAM	West African monsoon

List of contents

Publication list	i
Financial support.....	ii
Dedication	iii
Acknowledgements.....	iv
Resumo	v
Abstract	vi
Abbreviations and acronyms.....	vii
List of contents.....	ix
Figure index	xi
Table index.....	xiv
1. Introduction.....	1
1.1. Objectives of the work	3
2. Literature review	4
3. Materials and Methods.....	8
3.1. Study area.....	8
3.1.1. Topography	9
3.1.2. Climate characterization.....	9
3.2. Experiment setup.....	11
3.4. Data analysis	14
3.4.1. Inter-comparison between model's data and observational rainfall product	14
3.4.2. Historical droughts and humid periods in Cabo Verde.....	15
4. Results.....	18
4.1. West Africa precipitation: coupled versus uncoupled simulations	18
4.1.1. Seasonal precipitation	18
4.1.2. Absolute difference in seasonal mean precipitation between ROM and REMO	

4.2. Cabo Verde archipelago precipitation characteristics: Intercomparison between coupled and uncoupled simulations	22
4.2.1. Annual precipitation cycle	25
4.2.2. Rainfall interannual variability	30
4.2.3. Long term drought assessment.....	36
4.3. Added value of seasonal mean monthly precipitation	40
5. Discussion.....	44
6. Conclusions.....	47
7. Recommendations.....	49
8. References.....	50
Data availability.....	58

Figure index

Figure 1: Cabo Verde archipelago composition, topography and location in the context of West Africa(upper left side), followed by the regional division considered for the current study (Source: Vasconcelos et al., 2013): a) – north-western islands; b) - eastern islands and c) southern islands. On the right side is presented a satellite view of the archipelago highlighting the interaction between clouds and the topography.....	8
Figure 2: Major large-scale features such as the Intertropical Convergence Zone (ITCZ), Saharan Air Layer (SAL), African Easterly Jet (AEJ) and key synoptic and mesoscale weather systems of the West African Monsoon (Laing & Evans, 2011)	11
Figure 3: Model domain and orography [m] for REMO and ROM at a spatial resolution of 0.22° (red rectangle), and for MPIOM at a TR04 grid (black grid) (Weber et al., 2022).	13
Figure 4: Mean seasonal cycle of precipitation [mm/month] over West Africa from 1981 to 2010 of (a-d) Coupled simulation, (e-g) Uncoupled simulation and (i-l) CHIRPS for (a-e-c) December to February (DJF), (b-f-j) March to May (MAM), (c-g-k) July to August (JJA) and (d-h-l) September to November (SON).	19
Figure 5: Spatial distribution of mean precipitation over West Africa during Cabo Verde archipelago rainy season(August-September-October - ASO) for the time period of 1981–2010: (a) Coupled simulation, (b) Uncoupled simulation, both forced with ERA-Interim and (c) CHIRPS.	20
Figure 6: Absolute differences in seasonal mean precipitation [mm/month] over West Africa of (a-d) coupled minus uncoupled, (e-h) coupled minus CHIRPS over continent, and (i-l) uncoupled minus CHIRPS over continent for (a-e-c) December to February (DJF), (b-f-j) March to May (MAM), (c-g-k) July to August (JJA) and (d-h-l) September to November (SON) from 1981 to 2010.....	22
Figure 7: Seasonal means of precipitation in [mm/month] over Cabo Verde of (a-d) Coupled simulation, (e-g) Uncoupled simulation and (i-l) CHIRPS for (a-e-c) December to February (DJF), (b-f-j) March to May (MAM), (c-g-k) July to August (JJA) and (d-h-l) September to November (SON) from 1981 to 2010.	24
Figure 8: Spatial distribution of mean precipitation over Cabo Verde for the time period of 1981–2010 from left to right, in Coupled simulation (a), Uncoupled simulation (b), both forced	

with ERA-Interim and CHIRPS (c) during the country rainy season, August, September and October (ASO).25

Figure 9: Monthly mean precipitation over Cabo Verde islands for the period of 1981 to 2010 as simulated by the Coupled and Uncoupled models and observed by CHIRPS and two different combination of rain gauge: (a) using only low altitude stations (< 100 meters) and (b) combining low and high latitude stations.26

Figure 10: Relative monthly contribution to the total precipitation over Cabo Verde from rain gauge (low latitude stations) (a); CHIRPS (b); Coupled model (c) and Uncoupled model (d) from 1981 to 2010.....27

Figure 11: Monthly mean precipitation over Northern Islands (a), Southern Islands (b), Eastern Islands (c) for Coupled, Uncoupled, and CHIRPS for the period from 1981 to 2010.....29

Figure 12: Annual precipitation anomaly over Cabo Verde based on rain gauge (a), CHIRPS (b), Coupled model (c) and Uncoupled model (d); It is also added a 5-years moving average (black dashed line). Anomalies are with respect to the annual mean precipitation calculated for the 1981–2010 period.31

Figure 13: Annual precipitation anomaly over Northern Islands based on CHIRPS (a), Coupled model (b) and Uncoupled model (c): It is also added a 5-years moving average (black dashed line). Anomalies are with respect to the annual mean precipitation calculated for the 1981–2010 period.32

Figure 14: Annual precipitation anomaly over Southern Islands based on CHIRPS (a), Coupled model (b) and Uncoupled model (c): It is also added a 5-years moving average (black dashed line). Anomalies are with respect to the annual mean precipitation calculated for the 1981–2010 period.34

Figure 15: Annual precipitation anomaly over Eastern Islands based on CHIRPS (a), Coupled model (b) and Uncoupled model (c): It is also added a 5-years moving average (black dashed line). Anomalies are with respect to the annual mean precipitation calculated for the 1981–2010 period.35

Figure 16: Standard Precipitation Index 36-month calculated for Cabo Verde based on: CHIRPS (b), Coupled model (c) and Uncoupled model (d) datasets from 1981 to 2010.37

Figure 17: Standard Precipitation Index 36-month calculated for Northern Islands based on: CHIRPS (a), Coupled model (b) and Uncoupled model (c) datasets.38

Figure 18: Standard Precipitation Index 36-month calculated for Southern Islands based on: CHIRPS (a), Coupled model (b) and Uncoupled model (c) datasets.39

Figure 19: Standard Precipitation Index 36-month calculated for Eastern Islands based on: CHIRPS (a), Coupled model (b) and Uncoupled model (c) datasets.40

Figure 20: Added value AV of seasonal mean monthly precipitation for West Africa in ROM compared to REMO. Reference dataset is CHIRPS from 1981 to 2010 for December to February (DJF) (a), March to May (MAM) (b), July to August (JJA) (c) and September to November (SON) (d). Positive (negative) values indicate a lower (higher) precipitation bias of ROM compared to REMO.41

Figure 21: Added value AV of seasonal mean monthly precipitation for Cabo Verde in ROM compared to REMO. Reference data set is CHIRPS from 1981 to 2010 for December to February (DJF) (a), March to May (MAM) (b), July to August (JJA) (c) and September to November (SON) (d). Positive (negative) values indicate a lower (higher) precipitation bias of ROM compared to REMO.42

Figure 22: Added value AV of seasonal mean monthly precipitation for West Africa in ROM compared to REMO. Reference data set is CHIRPS from 1981 to 2010 for August September and October (ASO).43

Table index

Table 1: Overview of the performed model simulations	12
Table 2: Eleven rain gauge stations from the Cabo Verde National Institute of Meteorology used in the present study.	14
Table 3: Categories and scale of SPI index adapted from (Mckee et al., 1993).....	16

1. Introduction

Highly affected by the adverse effects of climate natural variability and climate change, West Africa is one of the most vulnerable regions to climate hazards. This is due to its low adaptive capacity to the observed and predicted climate changes (Akinsanola et al., 2018). Home to more than 400 million people, West Africa depends greatly on rain-fed agriculture and its natural resources to support food security and livelihoods.

West Africa's climate is strongly affected by the interaction of two air masses, one from the Atlantic Ocean and that from the Saharan desert. Both temperature and precipitation and their annual cycle are under the influence of the north-south movement of the Intertropical Convergence Zone (ITCZ). The dynamic of the ITCZ progression is made more complex by its interaction with another driver: the thermal heat low generated by the surface heating over the Sahara Desert (Lewis & C, 2016). In conjunction with the ITCZ, the West African monsoon (WAM), a reversing seasonal low-level circulation pattern, represents the region's main driver of rainfall variability.

The Intergovernmental Panel on Climate Change (IPCC) report emphasizes that climate change increases. It intensifies food shortage risks for countries and already vulnerable populations, with increased precipitation intensity and variability projected to increase flooding and drought risks (IPCC, 2021). Therefore, countries in this region must gain an understanding of climate, including its temporal and spatial variabilities. This knowledge is essential for assessing vulnerability and developing monitoring, forecasting, mitigation, and adaptation tools.

The context in which climate change occurs, and the vulnerabilities and the critical importance of climate to human and planetary well-being, push the demands on climate science to provide high-quality and traceable information. Climate models provide fundamental machinery to understand the processes supporting the variability and the long-term change in key meteorological parameters such as precipitation and temperature (Lewis & C, 2016). Climate models are the primary tool for assessing the projected future response of the atmosphere-land-ocean system to changing atmospheric composition (Schoof, 2013).

Scientists use Global Climate Models (GCMs) to study the behaviour and development of the Earth's climate over time. CMs can provide projections of how our planet's climate may change in the future. These GCMs projections are the main support for the international community to make climate change adaptation and mitigation decisions. However, the climate

change impacts, and the needed mitigation and adaptation strategies to tackle the impacts, will occur on more regional and national scales. Therefore, there is a requirement for climate change projections with much greater spatial detail and more accurate representation of regional climate and localized extreme events. In this context Regional Climate Downscaling (RCD) is crucial.

Defined as the use of GCMs simulations to force Regional Climate Models (RCMs), RCD can be applied over a limited area (Rummukainen, 2010) and has proved to be relevant in providing information on regional and local scales, therefore, supporting more detailed evaluation of climate change impact and adaptation assessment and planning (Fuhrer et al., 2014). This approach is vital in many vulnerable regions, mainly where interaction between regional and local scale processes strongly modulates climate conditions.

The use of regional atmosphere-ocean coupling in RCMs has been examined in numerous studies, which have demonstrated its advantages in a variety of applications. Research by (Cabos et al., 2019, 2020; Paxian et al., 2016; Sein et al., 2014) has demonstrated that the use of regionally-coupled model (ROM) can enhance the accuracy of key climate variables derived from global forcing models in simulations of current climate conditions. However, many RCD used to produce future climate change scenarios are still based on uncoupled simulations.

Heterogeneous and complex topography shapes small islands like Cabo Verde, whose climate conditions are subject to a significant impact of local and regional forcing, challenging GCMs with low spatial resolution. Cabo Verde's climate is a result of the interaction between its complex topography and the influences of both oceanic and West African continental processes. This, among other aspects, is a feature that GCMs cannot simulate, and high-resolution climate modelling is required.

There needs to be more studies focusing on these islands, despite all challenges highlighted by IPCC regarding the small states. Even with an important volume of regional downscaling studies focusing on WAM region, including within CORDEX framework, Cabo Verde Islands are often out of the regional model's domain.

Focused on the regional downscaling simulations of rainfall historic variability across Cabo Verde archipelago and the role of coupled ocean-atmosphere modelling, the main question driving the present work is:

- Is there added value in the Regional Climate Downscaling (RCD) simulations of historical precipitation over Cabo Verde region provided by regionally atmosphere-ocean-coupled model simulations compared with uncoupled RCD?

With the present research results, we expect to contribute to evaluating the current knowledge on the representation of precipitation variability across Cabo Verde. Specifically, we seek to evaluate the role of regionally coupled ocean-atmosphere modelling systems in providing better representation of precipitation patterns that can support and guide public policies that aim to tackle climate change challenges, namely those related to food and water security.

1.1. Objectives of the work

The main objective of the present work is to evaluate the impact of a regional atmosphere-ocean coupling model on the simulation of precipitation over Cabo Verde to achieve this main goal, the following specific objectives are to:

- Examine the simulate features of annual cycle of precipitation over West Africa and Cabo Verde domains by comparing coupled and uncoupled simulation runs against observations;
- As simulated by coupled and uncoupled models, assess the interannual variability of precipitation anomalies and long-term drought over Cabo Verde.
- Evaluate the added value of applying regional atmosphere-ocean coupling systems to simulate rainfall patterns across the country regions.

2. Literature review

Climate change has a far-reaching influence on natural ecosystems, the environment, and social economies. The future climate is likely to be significantly different from that of the present because of global warming owing to increased greenhouse gas emissions from human activities. Climate change scenarios are needed to assess the impacts of these changes on human activities and the environment (Fan et al., 2013). Global climate change influences extend to local and regional scales, which will be experienced by humankind directly. Simulating climate change, especially at regional scale, is very important for policy-making (Xu et al., 2019). The need for climate change information at the regional-to-local scale is one of the central issues within the global change debate (Giorgi et al., 2009). Fine-scale weather and climate information are urgently needed in many research areas, such as meteorology, hydrology, agriculture, ecology, renewable energy, and the atmospheric environment. In order to overcome this problem, various “regionalization” or “downscaling” techniques have been developed (Giorgi et al., 2009).

According to (Maurer & Hidalgo, 2008) downscaling is the process of converting information from a coarse-resolution climate model to a finer spatial resolution model. Downscaling techniques can be divided into two broad categories: dynamical downscaling and statistical downscaling (Fowler et al., 2008). The purpose of downscaling is to obtain high-resolution detail on essential climate variables such as precipitation as accurately as possible over the region of interest.

Currently, downscaling using GCM output is widely used to drive regional climate models (RCMs) because of their skill enhancement over GCMs due to their higher resolution and better representation of physical processes (Lo et al., 2008). The RCM is not intended to modify or correct the large-scale circulation of the Atmosphere Ocean Global Circulation Model (AOGCM) but is intended to add regional detail in response to regional scale forcing (e.g., topography, coastlines, and land use/land cover) as it interacts with the larger-scale atmospheric circulations (Gao et al., 2006). This method enables the simulation of many more variables and is not limited to locations with observational data. It also allows simulations of greater topographic complexity and finer-scale atmospheric dynamics, improving spatial resolution by 2–10 versus the global driving model. This capability could, in principle, allow modelers to represent information required for regional climate change studies and their impacts (J. Wang & Kotamarthi, 2015). In order to get finer-scale and higher-resolution

weather and climate information many GCMs have been downscaled by RCMs in the framework of large coordinated efforts in order to assess their potential for regional climate projection studies (Christensen & Christensen, 2007; van Ulden & van Oldenborgh, 2006; Jacob et al., 2014). It is important to state that these past efforts provided a new opportunity for the intercomparison of different models, initial and lateral boundary conditions, parameterization schemes, and grid resolutions (Jacob et al., 2007; Nikulin et al., 2012; Gbobaniyi et al., 2014; Sylla et al., 2013; Klutse et al., 2016). Because the model covers only a limited area, and it can reach very high horizontal resolutions RCMs have been shown to improve the simulation of climatic spatial detail (e.g., as forced by complex topography and coastlines) and extreme events compared to the driving global models (Giorgi, 2006).

The regional climate model (Jacob, 2001; Jacob et al., 2001) has been widely used in atmospheric researches. Previous evaluations have highlighted the model performance in terms of the basic features of regional climate over several domains (Jacob et al., 2012; Kumar et al., 2014), such as the African area (Paeth et al., 2009; Vondou & Haensler, 2017). However, RCMs have been developed and may meet various needs, the feedbacks related to atmosphere-ocean interactions and local processes that significantly impact the spatial and temporal structures of regional climate are not adequately taken into account in most climate models (D. Wang et al., 2006; Lucas-Picher et al., 2011). Therefore, the lack of representation of these interactions leads to inaccurate simulation of climate change in many regions, including small islands (Weber et al., 2022). That is why there is an increase development of regionally atmosphere-ocean coupled model.

In general terms, a regionally atmosphere-ocean coupled model is a modelling approach that focuses on estimating regional climate variability and its dependence on large-scale atmospheric and regional ocean circulations (Weber et al., 2022). This approach involves coupling a global ocean-sea ice model with a high-resolution atmospheric regional model and a global terrestrial hydrology model to divide the global ocean model setup into two different domains - one coupled where the ocean and atmosphere interact and another uncoupled where the ocean model is driven by prescribed atmospheric forcing and runs in a stand-alone mode (Sein et al., 2014). The model configuration influences the results of climate simulations and regional models can generate their own climate, with variability that can differ significantly from the prescribed climate of the global model. Thus, for regional climate modelling applications, an additional uncertainty associated with the extension of the model domain must be considered.

Based on the atmospheric REMO model, the regionally atmosphere-ocean-coupled model ROM (REMO-OASIS-MPIOM) has been developed to investigate the regional climate and local processes (Sein et al., 2014; Niederdrenk et al., 2016). Therefore, the explicit inclusion of the feedback between the atmosphere and ocean is necessary, many studies have looked at the benefits of using regional atmosphere-ocean coupling in Regional Climate Models (RCMs). These studies have shown that this approach can improve the accuracy of key climate variables when simulating current climate conditions. Specifically, the use of a regionally coupled model (such as ROM) can improve the accuracy of climate variables derived from global forcing models.

Looking at the benefits of simulating precipitation characteristics over Africa with a regionally-coupled atmosphere-ocean model Weber et al., (2022) found that the climate change signal of precipitation in the coupled simulation is more physically consistent due to the consideration of atmosphere-ocean interactions. By reducing the known SST warm biases in the tropical Atlantic and the Southwest Indian Ocean in climate models, Weber et al., (2022) were able to perform a more realistic simulated precipitation over most coastal regions of Sub-Saharan Africa. A northward displacement of ITCZ, due to colder SST, plays an important role in the observed impact of ROM.

Cabos et al., (2018) in their study which is based on dynamical downscaling with a regionally atmosphere-ocean coupled model over CORDEX Central America domain, showed that the coupled downscaling improves the representation of the Mid-Summer Drought and the meridional rainfall distribution in southernmost Central America. Over the regions of humid climate, the coupling corrects the wet bias of the uncoupled runs and alleviates the dry bias of the driving model, yielding a rainfall seasonal cycle similar to that in the reanalysis-driven experiments.

While simulating the East Asian summer monsoon (EASM), Zhu et al., (2020) found that in general, when compared with the standalone REMO model, ROM improves simulations of the circulation associated with the moisture transport in the lower- to mid-troposphere and reproduces the observed EASM characteristics, demonstrating the advantages of the regionally coupled model ROM in regions where air-sea interactions are highly relevant for the East Asian climate.

There have been few applications of REMO and ROM to West Africa, where the ocean conditions, especially in the North Atlantic, function as sources of both heat and moisture and

have substantial impacts on the local and surrounding atmospheric circulation systems (Zhang et al., 2015; Zu et al., 2019). The WAM and ITCZ are the most typical and important components of the climate in this region. Thus, the WAM, with its complex spatial and temporal structure, has received increasing attention. As refined numerical simulations of climatology in global models do not provide satisfactory results, it has been shown that atmosphere-ocean feedbacks have a crucial role in simulating the climate change (Zou et al., 2016).

Weber et al., (2022) used ROM to investigate the impact of atmosphere-ocean coupling on precipitation over several islands offshore the African continent since the SST of the surrounding oceans strongly affects the precipitation over the islands. The impact on the Cabo Verde archipelago was not evaluated in the Weber et al., (2022) study, which also works as a motivation to explore the impact of atmosphere-ocean coupling modelling on rainfall in Cabo Verde in the current study. For the analysed islands (e.g., Canary, São Tomé e Príncipe). Their results show that ROM simulates precipitation changes compared to REMO between -100 and $+100\%$ over the Canary Islands and between -100 and -25% over São Tomé and Príncipe. They explain the decrease (increase) in precipitation over the islands with the lower (higher) evaporation of moisture over the surrounding sea surfaces produced lower (higher) SST value. As recommendation, they indicate that simulation of precipitation over islands should either use bias-corrected SSTs of the surrounding oceans or use a regionally coupled atmosphere–ocean model.

3. Materials and Methods

3.1. Study area

Cabo Verde archipelago (Figure 1) is located in the eastern portion of tropical North Atlantic ($14^{\circ}50'–17^{\circ}20'N$, $22^{\circ}40'–25^{\circ}30'W$) about 750 km west of Senegal. It is composed of ten islands, nine of which are inhabited, and several uninhabited islets, divided into two groups by their location relative to the prevailing winds: the islands of Barlavento (windward) group the northernmost and easternmost islands, including the islands of Santo Antão, São Vicente, Santa Luzia (uninhabited), São Nicolau, Sal, Boavista and the Sotavento (leeward) group to the southernmost islands, formed from by Maio, Santiago, Fogo, and Brava. The total combined land area is about 4,033 square kilometers¹

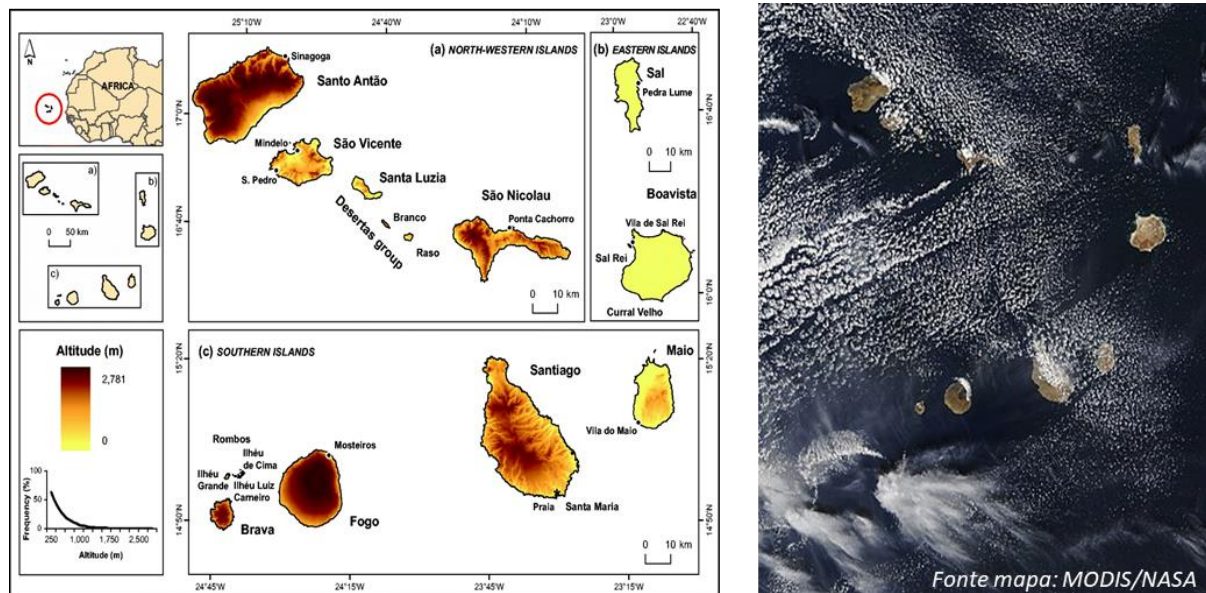


Figure 1: Cabo Verde archipelago composition, topography and location in the context of West Africa (upper left side), followed by the regional division considered for the current study (Source: Vasconcelos et al., 2013): a) – north-western islands; b) - eastern islands and c) southern islands. On the right side is presented a satellite view of the archipelago highlighting the interaction between clouds and the topography.

According to United Nation Population Fund (UNFPA), the population of Cabo Verde totals approximately 556,000 inhabitants in 2020². The Cabo Verdean economy is based on different services like commerce, transport, tourism, agriculture and public services. The services sector, particularly tourism, is the leading growth sector and has considerable potential for further diversification. The country's arable land is estimated at 10% of the total area and

¹ https://en.wikipedia.org/wiki/Geography_of_Cape_Verde

² <https://www.unfpa.org/data/world-population/CV>

is mainly concentrated on the major agricultural islands. 9% of this area is irrigated, and the rest is limited to rain-fed agriculture, being 19% in wetlands, 42% in sub-humid areas and 39% in arid areas. Of the total arable land, around 68% has rain fed crops vocation, 26% for agriculture, forestry, pastoral activities and 6% for irrigated crops in the alluvium of streams or slopes. The island of Santiago has approximately 58% of the land dedicated to agricultural soils, followed by Santo Antao, Fogo and São Nicolau (Government of Cabo Verde; MERD, 2010).

As a Small Island Development State (SIDS) with volcanic origin, Cape Verde presents a vulnerable environment system. The country is exposed to natural hazards, including extreme weather, floods, landslides, earthquakes, and volcanic eruptions. In addition, climate change, rainfalls, droughts, and soil degradation negatively impact biodiversity, access to water, agriculture, food security, and nutrition (World Bank-GFDRR, 2020).

3.1.1. Topography

Cabo Verde's islands generally have quite uneven topography, with steep, deep and ramified valleys (Figure 1). The land is generally hilly in younger islands, including the islands of Fogo, Brava, Santiago, Santo Antão and São Nicolau, culminating in very high altitudes (2829 m – Fogo; 1.979 m - S. Antão; 1.395 m – Santiago; 1.340 m - São Nicolau) and relatively flat in the older islands namely Sal, Boavista and Maio. Spatial dimensions and configurations of the topography, regarding its position to the prevailing winds, are different from one island to another, resulting in their wide-ranging landscapes. Such small-scale, complex and varied topography in Cabo Verde significantly impacts agriculture via local climate conditions definition, especially for precipitation (Mannaerts & Gabriels, 2000). This is a great challenge for climate simulations based on global models. Therefore, Cabo Verde conditions require initiatives of regional climate downscaling in order to provide tailored climatic information with a finer spatial resolution able to effectively support local mitigation and adaptation to climate changes impacts. The development of fine-resolution climate prediction is thus essential to comprehensively reveal the potential impacts of climate change on the Cabo Verde Archipelago.

3.1.2. Climate characterization

The archipelago of Cabo Verde belongs to the Sahel climatic zone and is characterised by an abridged rainy season, sometimes very short. The Barlavento Islands have an arid climate, receiving less than 100 millimetres of rain annually. In contrast, the southern islands receive

between 200 and 300 mm of rain, so their climate is semi-arid. In both groups of islands, in lowland areas and along the coasts, there are rare rains concentrated from August to October (and sometimes also in July), which is also the warmest time of the year³. Cabo Verde's annual average temperature is around 25° C for coastal areas, reaching 19° C in areas above 1,000 metres. The minimum values, between 20°c and 21° C, occur from January to April, and the maximum values of 26° C to 28° C in August-September (Government of Cabo Verde; MERD, 2010).

Alongside its complex topography, Cabo Verde Islands are influenced by various large scale and regional atmospheric systems and atmospheric-ocean interaction processes that determine the archipelago's climate. Figure 2 presents a conceptual map pointing to some of these elements and aspects. As a result of the Azores subtropical anticyclone, the prevalence of northeast winds and its interaction with ocean (leading to the cold ocean current from the Canary Islands) and topography in Cabo Verde is a central aspect of the country's climate. The equatorial low pressure belt seasonal displacement, expressed in the map via the ITCZ, plays a major role in Cabo Verde and West Africa as a whole rainfall season (Silva et al., 2011). Being frequently downwind of the continent, Cabo Verde climate is strongly influenced by atmospheric systems operating across West Africa, especially those propagating from east to west, such as the Saharan Air Layer (SAL), Easterly waves (EWs), African easterly jet (AEJ). Two other aspects are central to the West Africa Monsoon (WAM) and that are expected to influence regional climate patterns and therefore Cabo Verde climate, in particular its rainfall, are the Saharan Heat Low (SHL) and the northward moisture flux from the Equator in the Eastern Atlantic Ocean and Gulf of Guinea. The northward moisture flux that feeds rainfall across West Africa is a case of the role of ocean-atmosphere interaction in this region (Government of Cabo Verde; MERD, 2010).

The Azores subtropical high acts as a regulatory factor of Cabo Verde's weather and climate variability, by controlling daily basis and seasonal oscillation of the trade winds with maritime or continental features, especially during the dry months (November to June) (Ferdinand, 2021). During the West Africa Monsoon period (June to October), there is the northward displacement movement of the ITCZ, characterised by southeast winds and an increase in disturbances from the east, contributing to bringing precipitation further north, being August-September-October the rainiest months in Cabo Verde. Between December and February, the islands are recurrently affected by air masses from extratropical latitudes.

³ <https://www.climatestotravel.com/climate/cape-verde>

The Azores anticyclonic location and intensity influence the air masses that penetrate Cabo Verde throughout the year, but also via the Canary current that influences Cabo Verde, which moves with northeast flow along the West African coast towards the islands, thus contributing to soften temperatures in the region and eventually affect rain variability. In the middle of the ocean, affected by regional atmospheric processes strongly dependent on ocean-atmosphere interactions, we hypothesise that Cabo Verde climate simulations would benefit from atmosphere–ocean coupling simulations (Government of Cabo Verde; MERD, 2010).

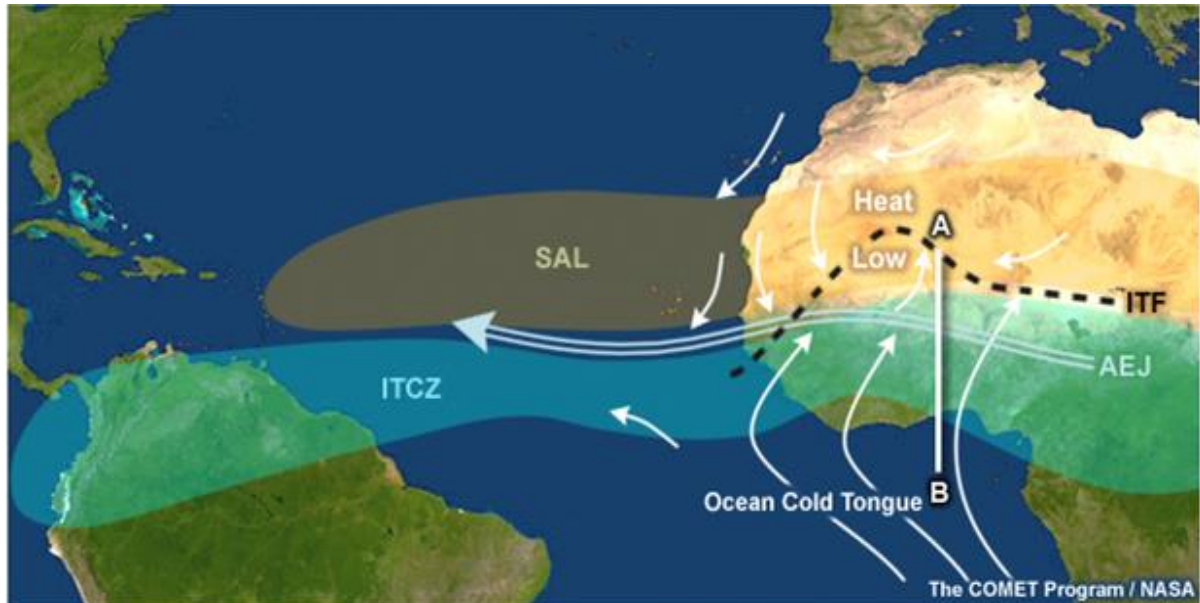


Figure 2: Major large-scale features such as the Intertropical Convergence Zone (ITCZ), Saharan Air Layer (SAL), African Easterly Jet (AEJ) and key synoptic and mesoscale weather systems of the West African Monsoon (Laing & Evans, 2011)

3.2. Experiment setup

As stated previously, the main goal of this study is to evaluate the benefits of atmosphere-ocean coupling in simulating historical spatiotemporal precipitation features for the Cabo Verde archipelago. This is done by comparing simulations from the regionally-coupled model ROM (Sein et al., 2015) and the atmospheric regional climate model REMO (Jacob et al., 2001). The dataset from ROM and REMO simulations used in this study were obtained from Climate Service Center Germany (GERICS) and are stored in the DKRZ archives⁴.

According to Weber et al., (2022), since REMO is the atmospheric component of ROM, it is possible to infer the benefits of atmosphere-ocean coupling by comparing their performance. ROM oceanic component is the Max Planck Institute Ocean Model (MPIOM; Marsland et al.,

⁴ <https://www.dkrz.de/en/systems/datenarchiv/datenarchiv-1-en>

2002 and Jungclaus et al., 2013), therefore ROM itself it is a result of a coupling between REMO and MPIOM via the OASIS coupler (Valcke, 2013), which provides exchange between the ocean and atmosphere models with a 3-h coupling time step. More details about the coupling procedure can be found in Sein et al., (2015). REMO’s dynamical core is based on the Europa Model from the German Meteorological Service and incorporates physical parameterizations from versions 4 and 5 of the ECHAM global climate model. For the simulations, REMO was configured with a horizontal grid of 0.22° (25 km), 31 vertical levels, and a 120 s time step. The model uses a regular rotated grid with the equator at the centre of the domain. The atmospheric domain chosen covers most of the tropical Atlantic (Figure 3), as well as parts of the Mediterranean and Indian Ocean, and is larger than the CORDEX-Africa domain. The MPIOM grid adjustment allows for high spatial resolution in the area of interest while keeping the global domain at a reasonable computational cost. The MPIOM TR04 grid has a horizontal resolution of up to 10 km near Western Africa’s coasts, gradually decreasing to 30 km near Africa’s southern tip and 100 km in the southern seas. Vertically, MPIOM has 40 unevenly spaced z-levels with thicknesses ranging from 16 m near the surface to 650 m for deeper layers.

Since the focus of this study is on the evaluation of the historical precipitation over Cabo Verde, the lateral boundary forcing is obtained from the ERA-Interim reanalysis for both the standalone and coupled cases. Which cover the period from 1981 to 2010, therefore setted the historical timeframe of the present study. A complete list of all models analysed can be found in Table 1.

Table 1: Overview of the performed model simulations

Experiment	Model	Forcing data	Period	Ocean-atmosphere
REMO/ERA-INT	REMO	ERA-Interim reanalysis	1981-2010	Uncoupled
REMO/ERA-INT	ROM	ERA-Interim reanalysis	1981-2010	Coupled

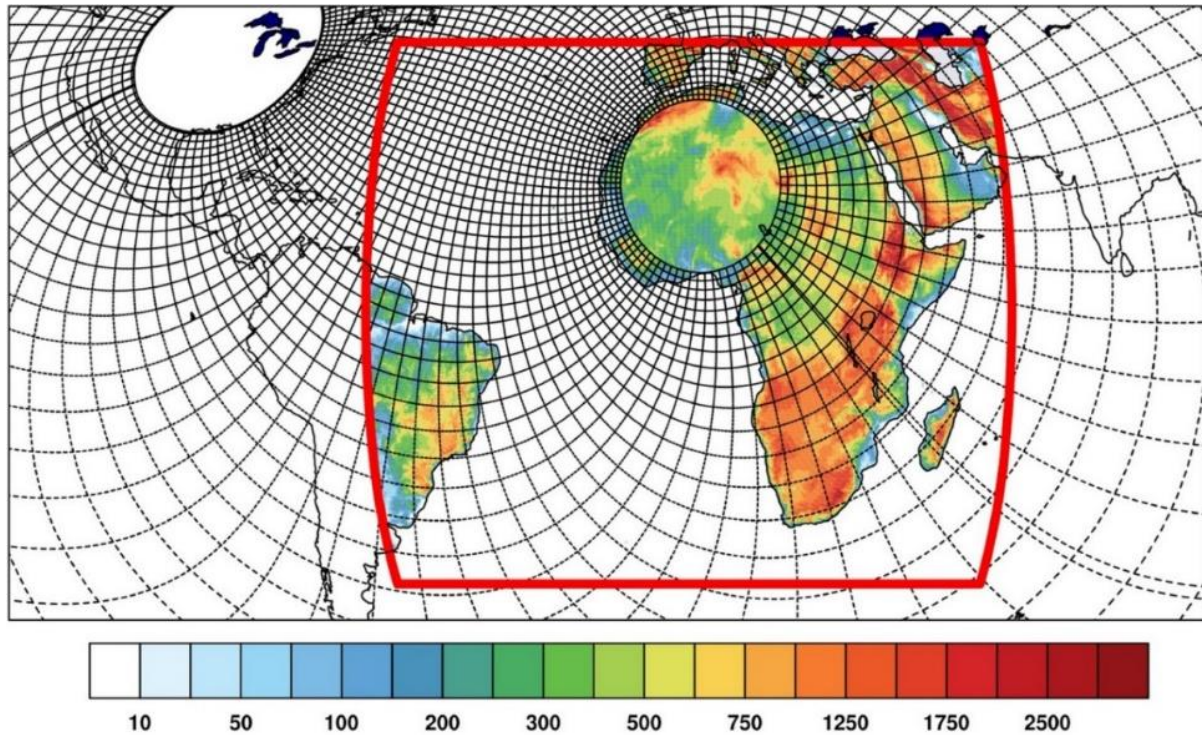


Figure 3: Model domain and orography [m] for REMO and ROM at a spatial resolution of 0.22° (red rectangle), and for MPIOM at a TR04 grid (black grid) (Weber et al., 2022).

3.3. Observational datasets

As an observational reference for evaluating the regional coupled and uncoupled modelling simulations over Cabo Verde, we used rain gauge data from reference stations belonging to Cabo Verde National Meteorological Institute (INMG) for the low-altitude stations and high altitudes. This separation between high- and low-level rain gauge stations meant to highlight the role of topography in rainfall spatial features in Cabo Verde. The stations names and locations are presented in Table 2. Also, precipitation product from the Climate Hazards Group InfraRed Precipitation with Station data (CHIRPS) which is a quasi-global rainfall dataset that has been developed by the Climate Hazards Center at UC Santa Barbara in collaboration with scientists at the USGS Earth Resources Observation and Science (EROS) Center. CHIRPS incorporates an in-house climatology that integrates 0.25° resolution satellite imagery and in-situ station data to create gridded rainfall time series for trend analysis and seasonal drought monitoring⁵.

⁵ <https://chc.ucsb.edu/data/chirps>

Table 2: Eleven rain gauge stations from the Cabo Verde National Institute of Meteorology used in the present study.

Station	Latitude	Longitude	Altitude
Mindelo, São Vicente	16,88	-25,00	10
Espargos, Sal	16,73	-22,95	54
Praia, Santiago	14,55	-23,29	64
S. Jorge dos Orgãos	15,03	-23,36	310
Babosa Picos	15,04	-23,37	454
Atalaia	15,01	-24,22	422
Galinheiro	15,59	-24,26	325
Ribeira ilheu	15,02	-24,22	362
Água das Caldeiras	17,12	-25,07	1433
Boca de Coruja	17,17	-25,12	145
Passagem	17,15	-25,05	330

3.4. Data analysis

3.4.1. Inter-comparison between model's data and observational rainfall product

In order to perform a comprehensive overview of the potential benefits of the regional atmosphere-ocean coupling in simulation of precipitation and its characteristics over Cabo Verde, 3 sub-domains were considered in the analysis. With the goal of providing a regional perspective of the benefits, the first domain analysed includes the Eastern tropical Atlantic and the entire West Africa. With this domain we target to evaluate ITCZ position and intensity in terms of associated rainfall and precipitation over the continental region. The second domain encapsulates just Cabo Verde Archipelago aiming to present an evaluation of the country rainfall mean features. For the 3rd domain reference, the country was split into 3 main regions as represented in Figure 1: Northern region (islands of Santo Antão, São Vicente, Santa Luzia and São Nicolau), Eastern region (islands of Sal and Boavista) and Southern region (islands of Maio, Santiago, Fogo and Brava). This separation recognizes the importance of the island's geographical disposition in relation to the prevalent wind and precipitation driven system. For instance, the southern islands are more affected by ITCZ than the northernmost islands. Eastern

islands, due to their flat topographical conditions, have no contribution of orographic precipitation in their pluviometry regime, as is the case of southern and northern islands.

Regarding temporal variability, the analyses were mainly focused on the seasonal and interannual variability, which was based on rainfall anomalies. Furthermore, we assess the benefits in simulating precipitation over Cabo Verde Island and West Africa using the regional atmosphere–ocean coupling by measuring the Added Value and selecting as observational reference of the rainfall product from CHIRPS.

In order to quantify the ability of the ROM to improve (or not) seasonal rainfall simulation over REMO results, we used the Added Value (AV) formula based on (Dosio et al., 2015), adapted from (Di Luca et al., 2012) (Eq.1):

$$AV = \frac{(REMO - REF)^2 - (ROM - REF)^2}{Max((REMO - REF)^2, (ROM - REF)^2)} \quad (Eq. 1)$$

Where:

- REF represents the reference dataset;
- AV is positive where ROM square error is smaller than REMO square error;
- The normalization is introduced so that the added values ranges from -1 to + 1.

Positive values indicate a lower precipitation bias of ROM compared to the bias of REMO, while negative values indicate a higher precipitation bias of ROM compared to the bias of REMO. Specifically, an AV of +1 means that the precipitation bias of the coupled model is zero, while an AV of -1 means that the precipitation bias of the uncoupled model is zero.

3.4.2. Historical droughts and humid periods in Cabo Verde

To understand ROM and REMO ability to reproduce the observed characteristics of persistent droughts and humid periods in Cabo Verde and to identify potential benefits of ocean-atmosphere coupling we used the standardised precipitation index (SPI, Mckee et al., 1993) as a metric for wet and dry periods identification.

There are several indices to monitor drought in the literature, Palmer Drought Severity Index (PDSI, (Palmer, 1965), the Standardized Precipitation Index (SPI, Mckee et al., 1993) and Standardized Precipitation Evapotranspiration Index (SPEI, Stagge et al., (2015). Their importance as tools to support public policies, agricultural systems monitoring, and study

climate variability and trends has been largely recognized (Nandintsetseg & Shinoda, 2013; Parry et al., 2016). For the present study, SPI was selected for its simplicity; it is a simple measure of drought and wet periods and considers only precipitation data as input, which is a differential in relation to the other indices. SPI quantifies the deficit or excess rainfall at different time scales, allowing the monitoring of short and long-term droughts (Mckee et al., 1993). Usually calculated for 1 to 36 months, it evaluates the dry and wet periods characteristics. Targeting persistent drought and wet periods we selected to analyse SPI-36, since they are associated with hydrological droughts (Abatan et al., 2017). The SPI calculation is based on the density and probability function Gamma (Eq. 2).

$$F(x) = \sum_0^x f(x)dx = \frac{1}{\Gamma(\alpha)\beta^\alpha} \int_0^x x^{\alpha-1} e^{-x/\beta} dx \quad (Eq. 2)$$

Where:

- $F(x)$ is the general formula for the probability density function of the exponential distribution;
- $\alpha > 0$ and $\beta > 0$ are, respectively, the form and scale parameters;
- $\Gamma(\alpha)$ is the gamma function;
- x is the rainfall amount, with x varying according to α and β .

The SPI values represent the number of standard deviations from the mean at which an event occurs. Thus, for instance, the 36-months SPI value compares accumulated rainfall over that specific 36-months period with the mean accumulated rainfall for the same period calculated over the full study period (Guenang & Mkankam Kamga, 2014). This applies to any n-month SPI value, where n, the number of months of accumulation, is the time scale. Persistence of high SPI positive values indicate wet conditions, and persistence high negative values correspond to drought scenarios. According to (Guttman, 1998), time scales on the order of 36 months are fitted to evaluate drought scenarios (negative SPI) for water-supply management. SPI categories of dryness and wetness events that are followed in this study are those based on the information presented in Table 3.

Table 3: Categories and scale of SPI index adapted from (Mckee et al., 1993)

SPI	Class
≥ 2	Extremely wet
1.50 to 1.99	Very wet
1.00 to 1.49	Moderately wet
0.99 to -0.99	Near normal
-1.50 to -1.49	Moderate drought
-1.50 to -1.99	Severe drought
≤ -2	Extreme drought

To compute SPI at the selected time scales (36 months) from all the precipitation time series (ROM, REMO, Rain Gauge and CHIRPS) over land area of Cabo Verde and following the regional separation (northern Islands, eastern Islands, and southern islands), an SPI function program developed for MATLAB software was used.

4. Results

4.1. West Africa precipitation: coupled versus uncoupled simulations

This section analyses mean spatial and seasonal precipitation variability over West Africa from 1981 to 2010, comparing a regionally coupled ocean-atmosphere model (ROM) and a regional atmospheric model (REMO) driven by ERA-Interim reanalysis. The analysis also includes comparisons between both model simulations against observational precipitation from CHIRPS. As already stated, this analysis's main goal is to provide an insight into the role of atmosphere-ocean coupling on the West Africa precipitation patterns before a more specific discussion focusing on the Cabo Verde islands.

4.1.1. Seasonal precipitation

The mean spatial features of seasonal precipitation cycle in West Africa for ROM, REMO and CHIRPS are presented in Figure 4. Although with some relevant differences, that will be discussed later, it can be inferred that both simulations reproduce the seasonal march of precipitation across West African. The peak of precipitation in the region is observed during June, July and August (JJA), consistent with the CHIRPS data and literature revision for the region (e.g., Janicot et al., 2011), with mean precipitation varying between 300 to 350 mm per month in both ROM (coupled simulation, Figure 4c) and REMO (uncoupled simulation, figure 4g). The driest period in West Africa, from December to February, is consistently represented in both simulations, with ITCZ rainfall belt further south. Based on this broad analysis, one can say that the West Africa precipitation seasonal march is represented in both simulations, coupled and uncoupled, following a similar pattern in terms of spatial distribution. However, is clearly visible that the amount of precipitation simulated over the ocean is lower in the coupled - ROM (Figure 4a-d) when compared to the uncoupled - REMO results (Figure 4e-h).

The results show that it rains in some areas between 10°N and 5°S of the Atlantic Ocean as well as along the West African coast during three seasons (March, April, May (MAM), JJA, September, October, November (SON)), with rainfall up to 300 mm per month recorded in the seasons of MAM and SON. The average seasonal precipitation in the northern regions of West Africa and the northern part of the Atlantic Ocean is relatively low in both ROM and REMO simulations. This is in contrast to the southern regions of West Africa, where precipitation levels are higher. Furthermore, the oceanic and coastal areas tend to receive more precipitation than the continental regions' interior.

Figure 4i–l represents the spatial distribution of seasonal precipitation for CHIRPS which cover only the continent. The season of JJA (Figure 4k) records the highest precipitation over the West African region. Also, precipitation occurs over the southern part of West Africa during three seasons (MAM, JJA, SON). The rainy season ends quickly over the northern regions of West Africa, when the ITCZ starts retreating down south to Central Africa.

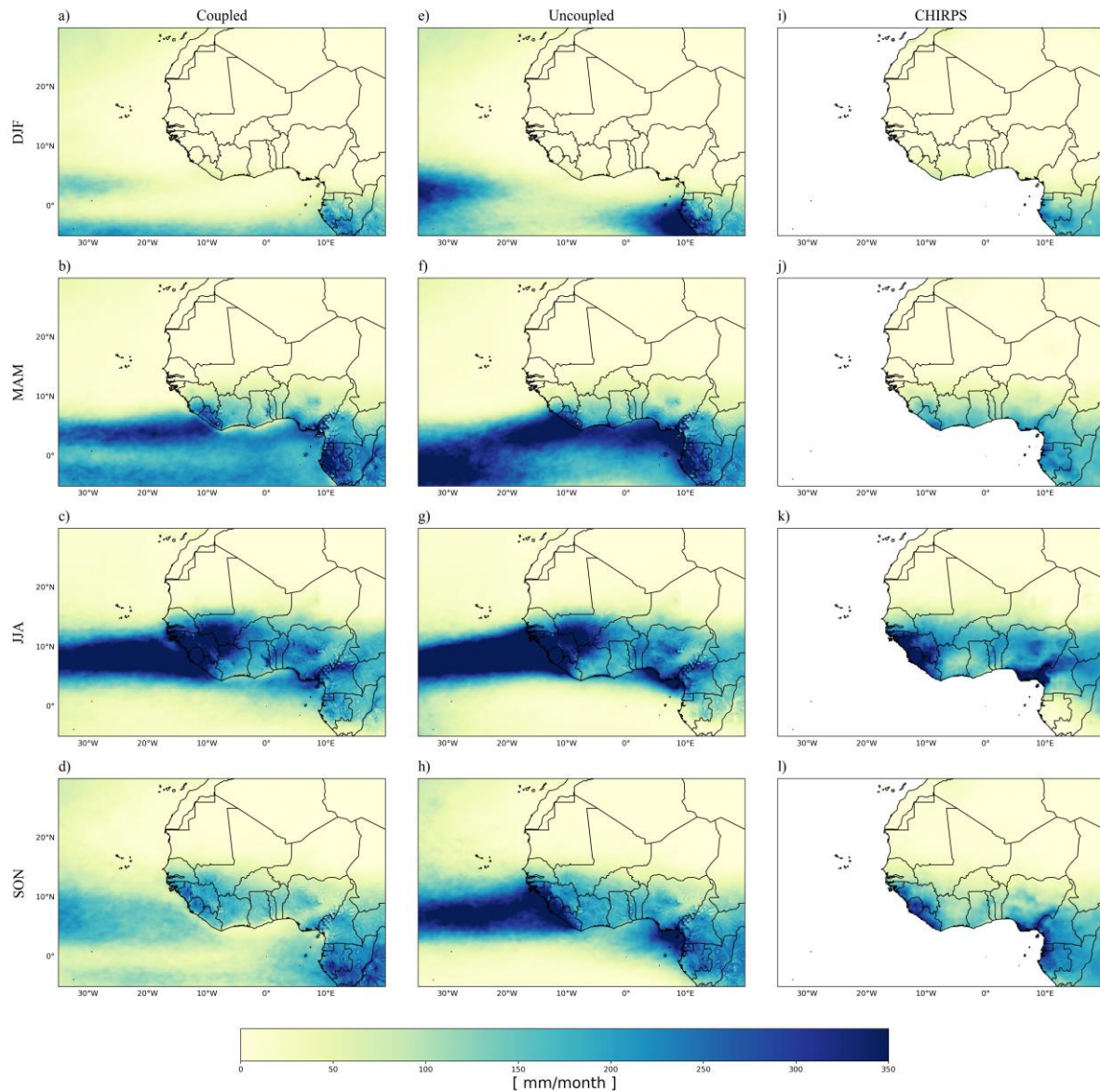


Figure 4: Mean seasonal cycle of precipitation [mm/month] over West Africa from 1981 to 2010 of (a-d) Coupled simulation, (e-g) Uncoupled simulation and (i-l) CHIRPS for (a-e-c) December to February (DJF), (b-f-j) March to May (MAM), (c-g-k) July to August (JJA) and (d-h-l) September to November (SON).

Figure 5 shows the results of the analysis of precipitation over West Africa for the Cabo Verde archipelago rainy season, which covers the months of August, September, and October (ASO); it reveals similar spatial distribution patterns for the Coupled (figure 5a) and Uncoupled

(figure 5b). The ITCZ rainbelt north border is just positioned southward of Cabo Verde Island domain. However, it is observed that the uncoupled simulation shows a higher amount of precipitation compared to the Coupled simulation. Another noteworthy difference observed is the strong concentration of rain belt at the core of the rainbelt over the Atlantic in the uncoupled simulation, which presents a sharp dilution as one moves northward or southward, while for the rainbelt simulated by the coupled model rain is more homogeneous its dilution towards south and north is gradual.

As noted, before, over land, the rainfall from both models (coupled and uncoupled) is generally consistent with that estimated in CHIRPS data. However, while uncoupled simulation seems to overestimate precipitation along the Guinea and Sierra Leone coast, both models overestimate precipitation over the southern of Mali and North of Côte d'Ivoire.

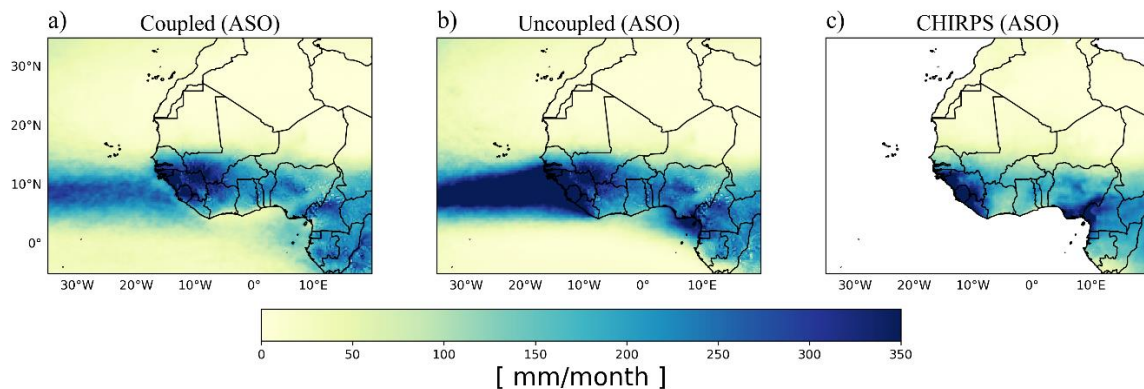


Figure 5: Spatial distribution of mean precipitation over West Africa during Cabo Verde archipelago rainy season (August-September-October - ASO) for the time period of 1981–2010: (a) Coupled simulation, (b) Uncoupled simulation, both forced with ERA-Interim and (c) CHIRPS.

4.1.2. Absolute difference in seasonal mean precipitation between ROM and REMO

Figure 6 shows absolute differences in seasonal mean precipitation between models and the observational dataset, indicating changes in precipitation values over West Africa. The difference between the Coupled and Uncoupled simulations (Figures 6a-d) is relatively low over most of West Africa during DJF (Figure 6a). This is mainly due to the fact that DJF comprises the dry season. Further south, over the Atlantic until Gabão and Guine Equatorial coast, the equatorial rain belt in coupled simulations produces less rain than the uncoupled model. Overland, even over rainy regions, coupled and uncoupled in general produce a similar amount of rain during DJF. However, differences become more noticeable during MAM (Figure 6b), with a decrease of around -40 to -80 mm/month in the coupled simulation over the

south coast of West Africa and Gulf of Guinea, when compared with uncoupled, while an increase of around 20 to 40 mm/month over the continent around Sierra Leone and Guinea regions. Over the Atlantic, in MAM, coupled simulation also produced less precipitation than uncoupled across most of the equatorial rain belt. Still at this time the negative values are flanked by two regions of positive values, indicating a larger extension of the equatorial rain belt in the coupled simulation. During JJA (Figure 6c), it is still possible to see a decrease of around -40 to -60 mm/month in precipitation over the ocean in coupled model compared with uncoupled, but the negative values belt it is compressed and shifted to north of the equatorial region connecting to the coast from Senegal to Liberia. This is a response to the seasonal displacement of the ITCZ rainbelt. Meanwhile, coupled simulation presents an increase of around 5 to 20 mm/month over land across West Africa in comparison to the uncoupled model. This feature change for SON (Figure 6d), which comprises the most important month of the rainy season in Cabo Verde (September), shows a decrease of around -40 to -80 mm/month in precipitation in the Coupled simulation both over the southern part of West Africa and over the ocean, even further north including Cabo Verde archipelago.

The results of coupled and uncoupled simulations masked over land areas minus observed rainfall (CHIRPS) are shown in Figures 6e-h and 6i-l, respectively. The difference between the Coupled simulations and CHIRPS (Figures 6e) and between Uncoupled simulations and CHIRPS (Figure 6i) is relatively low over most of West Africa during DJF. Both model results underestimate precipitation mainly over the south humid portion of the region, but this period is the dry season, therefore rain is scarce in most of West Africa. However, differences become more noticeable during MAM (Figure 6f and 6j), with an increase of around 40 to 60 mm/month in the coupled and uncoupled simulations over the south coast of West Africa and Gulf of Guinea, when compared with CHIRPS, while a decrease of around -5 to -20 mm/month over the continent around Sierra Leone and Guinea regions. The most significant increase is observed during SON (Figure 6g and 6k), where western part of West Africa experiences an increase in precipitation ranging from around 60 to 80 mm per month. During SON (Figure 6h) it is observed a decrease of around -40 to -60 mm per month in precipitation in the coast of West Africa from Guinea to Nigeria while an increase of around 40 to 80 mm per month is observed over the continent south to the Sahara when compared to CHIRPS. Figure 6l shows increased in precipitation in the uncoupled simulations compared to CHIRPS in a large part of West Africa.

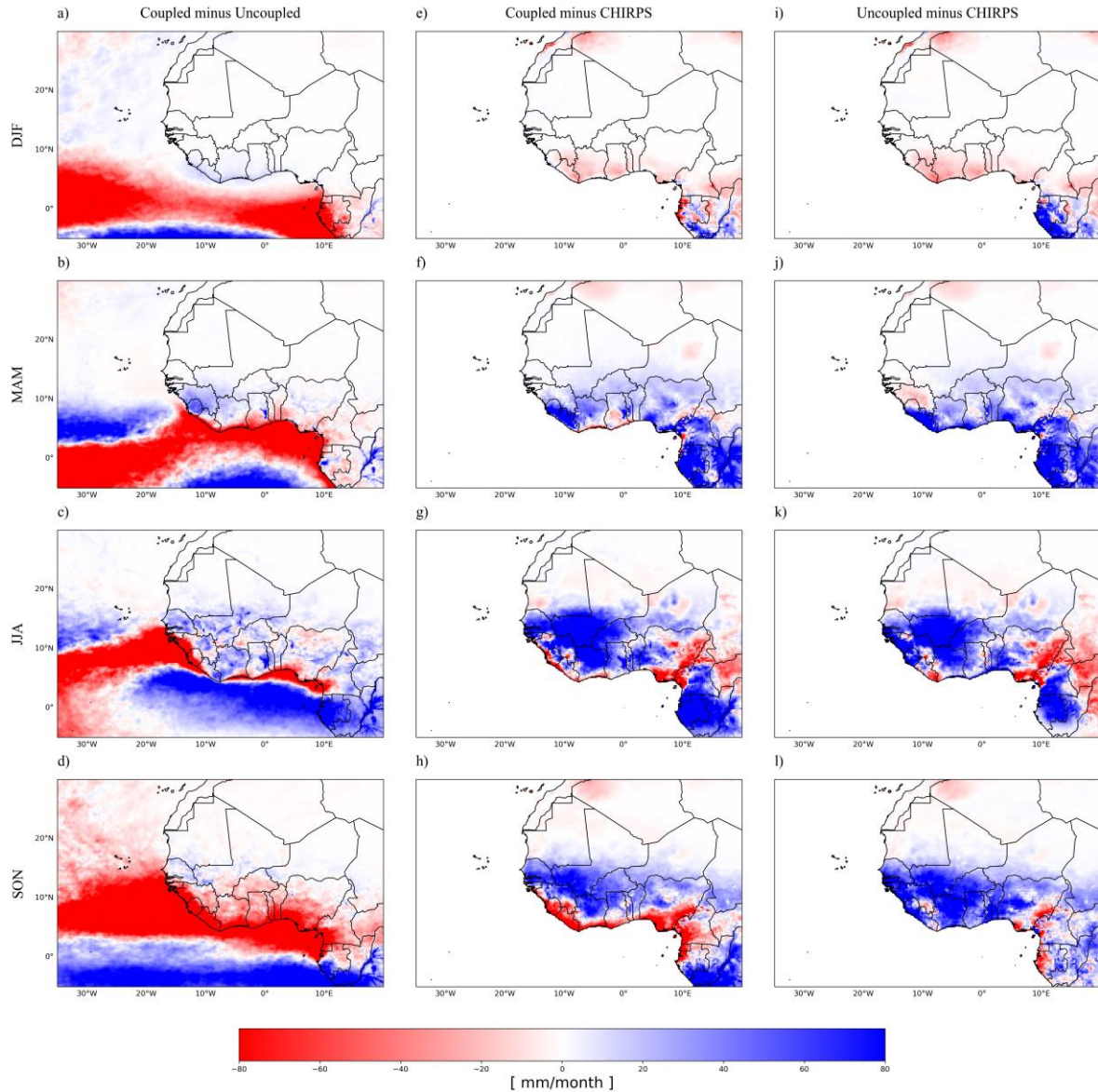


Figure 6: Absolute differences in seasonal mean precipitation [mm/month] over West Africa of (a-d) coupled minus uncoupled, (e-h) coupled minus CHIRPS over continent, and (i-l) uncoupled minus CHIRPS over continent for (a-e-c) December to February (DJF), (b-f-j) March to May (MAM), (c-g-k) July to August (JJA) and (d-h-l) September to November (SON) from 1981 to 2010.

4.2. Cabo Verde archipelago precipitation characteristics: Intercomparison between coupled and uncoupled simulations

This section analyses the seasonal and interannual precipitation variability over Cabo Verde archipelago and for the three specific regions according to the island's geographical disposition (Northern, Eastern, and Southern Islands) for the 1981 to 2010 period. To this end, rain gauge measurements from National Meteorological Institute, and precipitation field

(masked only for Cabo Verde land domain) from CHIRPS from coupled and uncoupled simulations were used. In order to compare the model's performance to reproduce Cabo Verde rainfall features, time series from both coupled and uncoupled simulations and CHIRPS over the entire Cabo Verde and for the three subregions were extracted and analyzed.

Figure 7 describes the mean seasonal cycle of precipitation distribution across Cabo Verde considering the study period of 30 years. Generally, according to the observation, precipitation increased spatially from north to south in Cabo Verde, which can be explained by the southern island's topography (mainly Fogo and Santiago) and southward position (therefore, more likely to be affected by ITCZ). This spatial pattern appears to be simulated consistently by both coupled and uncoupled. The archipelago generally experiences dry conditions in DJF (Figure 7a, 7e and 7i) and MAM (Figure 7b, 7f and 7j). The onset of wet season occurred around JJA (20–40 mm per month), mainly in the Southern Islands (Figure 7c, 7g and 7k), and then the rainfall spreads through the eastern and northern Islands to reach its peak in SON (Figure 7d, 7h and 7l). In general, higher precipitation amounts (40-70 mm per month) tend to occur during the SON throughout the country, but with the northern and eastern Islands receive lower amounts of precipitation (20-40 mm per month) compared to the southern islands. Coupled and uncoupled simulations capture all these timing features. However, uncoupled produce more rain than coupled throughout the country at the peak of rainy season (SON), while coupled produce higher amounts of rainfall at the beginning of wet season (JJA) for the southern islands. Both simulations produce higher rainfall when compared with CHIRPS data.

Focusing on the months that present the highest contribution to the rainy season, Figure 8 illustrates the mean precipitation during August, September, and October over Cabo Verde. The simulated rainfall, coupled and uncoupled, demonstrated a similar spatial distribution of precipitation across the country. The precipitation amount decreased from Southern to the Northern Islands. Therefore, model outputs were able to reproduce the amount even higher as registered in CHIRPS data. The highest amount of precipitation (60-90 mm per month) was observed over Southern Islands, while the lowest amount (0-40 mm per month) was observed in the Northern and Eastern Islands. Comparison between the datasets reveals that the coupled simulation (Figure 8a) improved the rainfall amount for every region as observed in CHIRPS (Figure 8c).

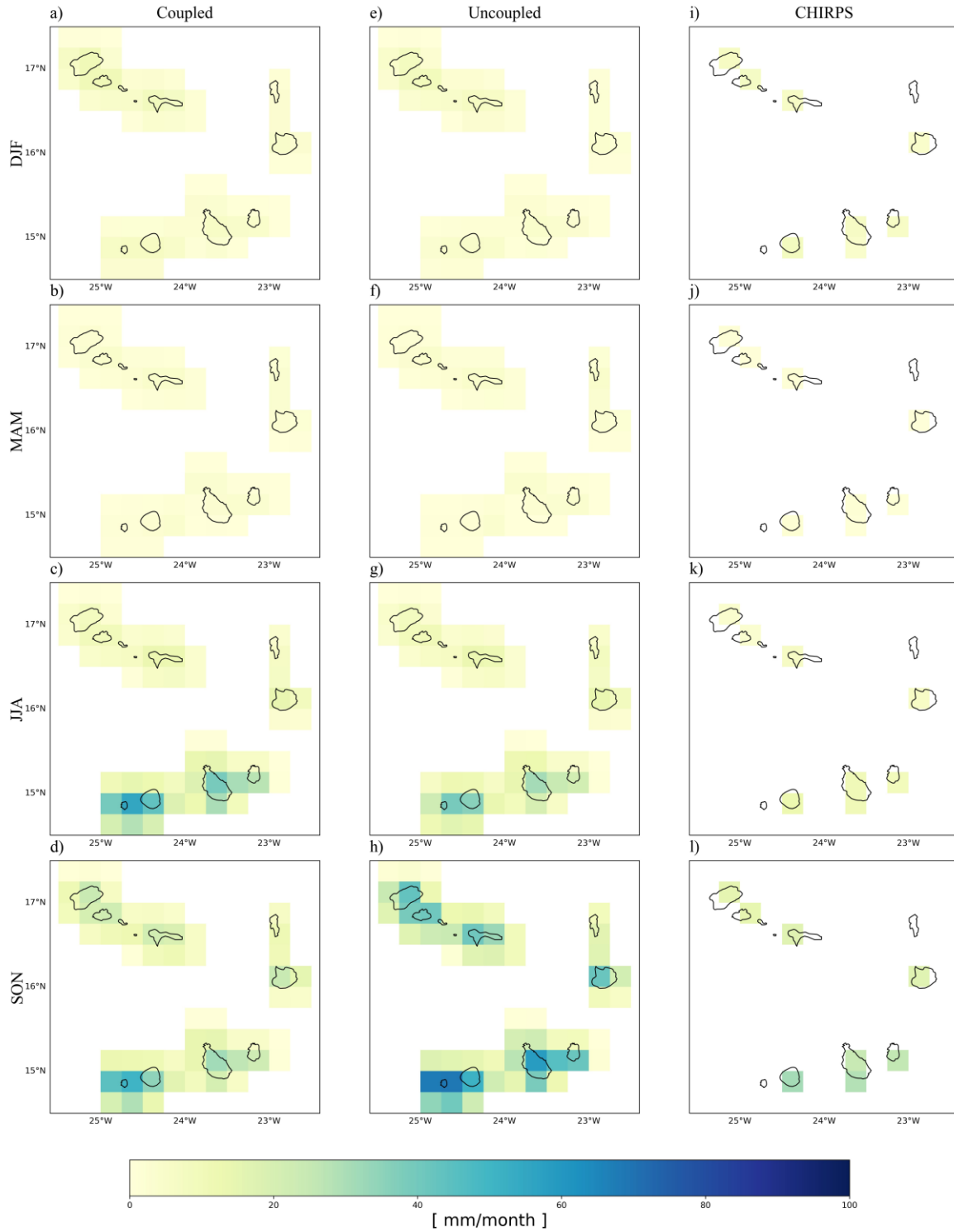


Figure 7: Seasonal means of precipitation in [mm/month] over Cabo Verde of (a-d) Coupled simulation, (e-g) Uncoupled simulation and (i-l) CHIRPS for (a-e-c) December to February (DJF), (b-f-j) March to May (MAM), (c-g-k) July to August (JJA) and (d-h-l) September to November (SON) from 1981 to 2010.

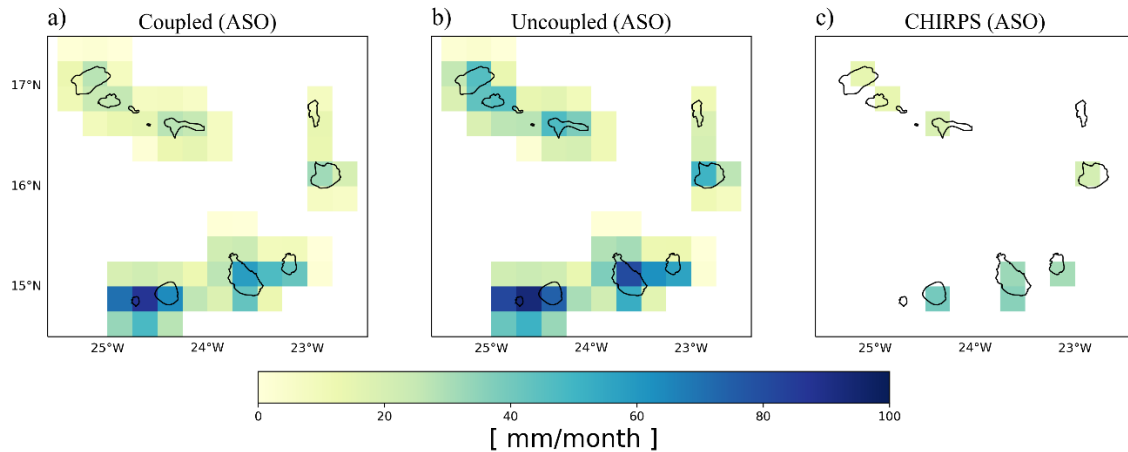


Figure 8: Spatial distribution of mean precipitation over Cabo Verde for the time period of 1981–2010 from left to right, in Coupled simulation (a), Uncoupled simulation (b), both forced with ERA-Interim and CHIRPS (c) during the country rainy season, August, September and October (ASO).

4.2.1. Annual precipitation cycle

To fully explore the consistency among the different datasets, the annual precipitation cycle assessment was conducted over Cabo Verde a whole and for the three subregions for the entire time period. The goal is to compare coupled and uncoupled simulations of precipitation for the entire country and sub-domains within the country, and CHIRPS and rain gauge precipitation are used to evaluate the precipitation from the models for these different domains. Figure 9 presents the average annual precipitation cycle from the three different datasets (Coupled, Uncoupled and CHIRPS) and rain gauges for the low altitude stations (Figure 9a) and rain gauges considering stations from both low and high altitude. This separation between high- and low-level rain gauge stations is meant to highlight the role of topography in rainfall spatial features in Cabo Verde. Consistently, in all data the precipitation volume in Cabo Verde increases from June, reaches its peak in September, and decreases toward October, until the end of the rainy season. However, there are differences in the amount of the precipitation. The mean annual precipitation cycle from stations at low level (< 100 meters) and CHIRPS show stronger consistency in both variability and amount, with the rainiest month (September) presenting rainfall values up to 40 mm. Although the peak of precipitation in the coupled model is closer to the low-level rain gauge and CHIRPS, it seems to produce less rain in September and October when compared with observations. The differences between precipitation field from coupled and that from uncoupled for JJA (Figure 6) show that coupled produced more rain around Cabo Verde at the beginning of the rainy season, indicating a northward displacement of Inter Tropical Convergence Zone (ITCZ) in the coupled run. Weber et al.,

(2022), found a similar change in the meridional precipitation pattern over West Africa in JJA, which shows a decrease in the South and an increase in the North. They suggest that the ITCZ moves further northward in the simulation with the regional coupled atmosphere–ocean model ROM than in uncoupled model REMO due to a colder SST in the Gulf of Guinea.

It is observed that when compared to the mean precipitation over Cabo Verde based on rain gauge, considering low and high-altitude stations (Figure 9b), CHIRPS, Coupled and Uncoupled simulations underestimate the rainfall in Cabo Verde.

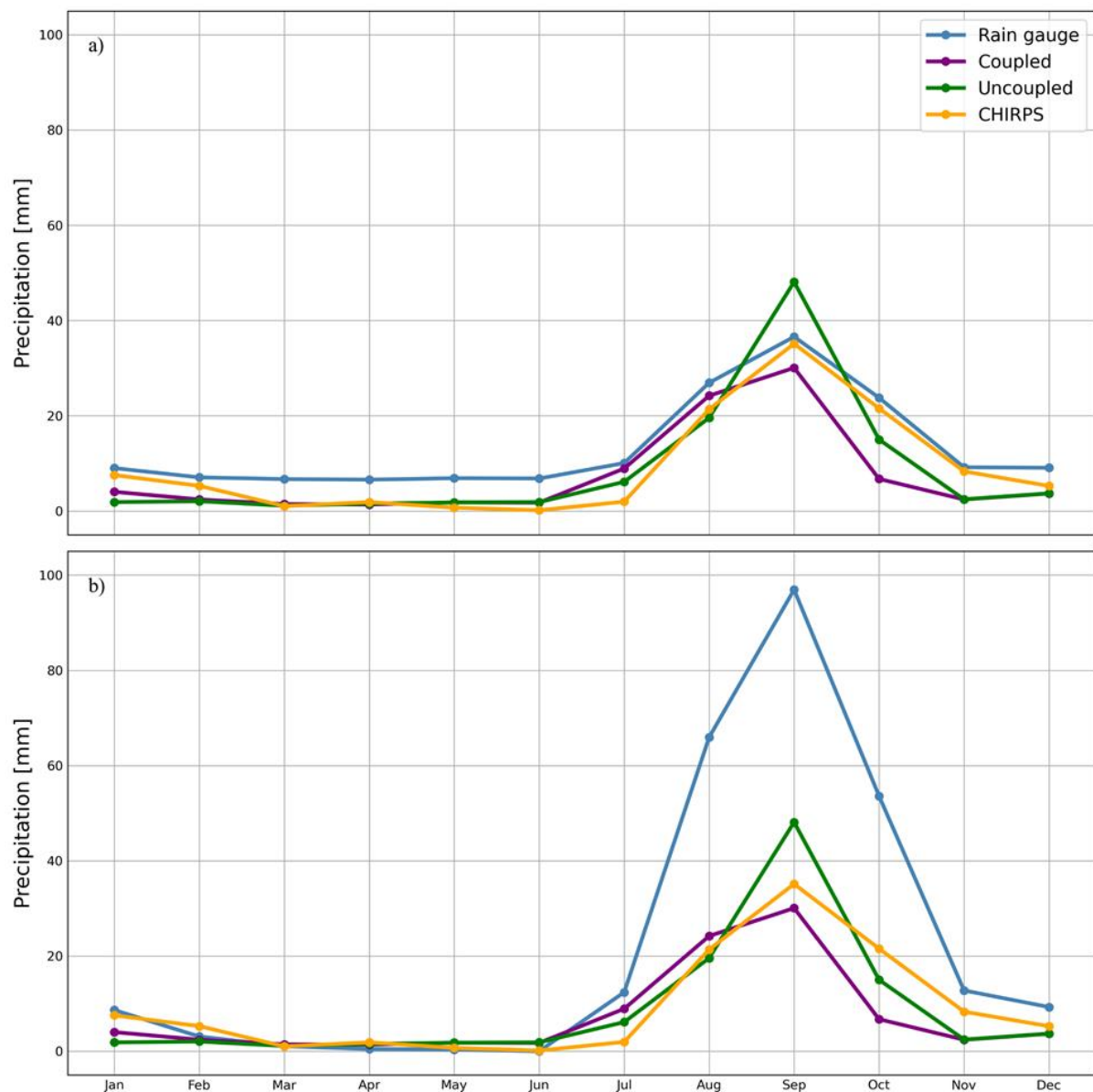


Figure 9: Monthly mean precipitation over Cabo Verde islands for the period of 1981 to 2010 as simulated by the Coupled and Uncoupled models and observed by CHIRPS and two different combination of rain gauge: (a) using only low altitude stations (< 100 meters) and (b) combining low and high latitude stations.

Figure 10 shows the relative contribution of each month to the total annual precipitation as observed and simulated by coupled and uncoupled models and observed by CHIRPS and low altitude rain gauges. Most of the precipitation over Cabo Verde occurs during August, September and October, with the rainfall of these months accounting for more than 50 % and 65% of precipitation according to rain gauge (low altitude stations) and CHIRPS, respectively. Coupled model produced 58 % for these 3 months. Meanwhile, the uncoupled model produced on average 70% of rainfall in August-September-October, higher to the observations and coupled model which is explained by the fact that it is overestimating significantly the contribution of September. Therefore, the coupled model can reproduce the contribution of the rainy season (ASO) to the total annual precipitation closer to the observation than the uncoupled model, the later one provided the worst intraseasonal distribution of the rainfall.

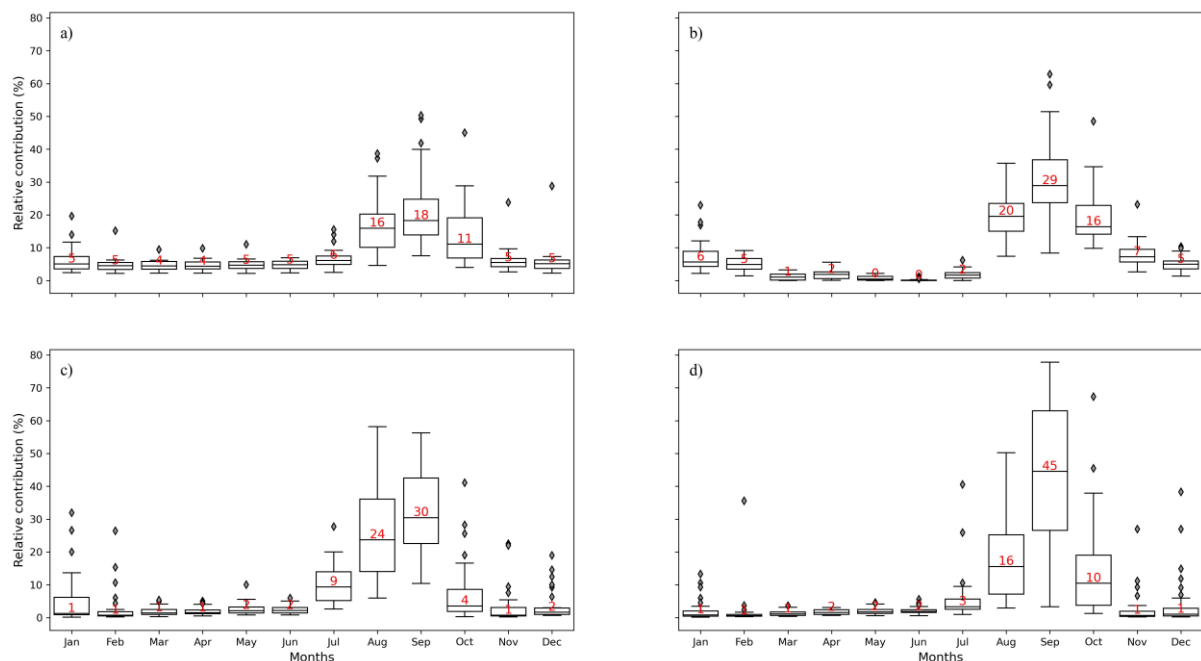


Figure 10: Relative monthly contribution to the total precipitation over Cabo Verde from rain gauge (low latitude stations) (a); CHIRPS (b); Coupled model (c) and Uncoupled model (d) from 1981 to 2010.

The monthly mean precipitation over the three subregions (Northern, Southern, and Eastern Islands) includes the three datasets, from CHIRPS, coupled and uncoupled simulations is presented in Figure 11. This information provides more detailed insights into the precipitation patterns in Cabo Verde and helps to evaluate models' ability to reproduce the known spatial distribution of rainfall across the archipelago.

According to the results presented in Figure 11, precipitation volumes begin to increase in July, peak in September, and then decrease towards October in all three localities. The Southern

Islands had the highest mean precipitation, with around 70 mm per month, while the Eastern Islands had the lowest mean precipitation, with less than 25 mm per month. The Northern Islands, where larger differences were observed between coupled, CHIRPS and uncoupled, present a mean rainfall amount in the rainiest month up to 60 mm in the uncoupled model. In general, the Coupled model was able to improve the annual cycle of precipitation in all the regions. The main contribution was its ability to reduce the unrealistic amount of precipitation simulated by the Uncoupled model at the peak of the rainy season. In the Northern Islands, the coupled model accurately captured the monthly precipitation cycle. However, it consistently underestimated the amount of precipitation in October, bringing an earlier end to the rainy season (as shown in Figure 11a) when compared to CHIRPS. Figure 11c shows the results for the Eastern Islands and reveals that the degree of consistency between the coupled model and CHIRPS data in reproducing the mean annual cycle of precipitation in this region is not better than that of the uncoupled model. Despite the improvement produced in the Southern Islands compared to the uncoupled simulations, the coupled model did not accurately capture the monthly mean distribution of precipitation. During July, and August the model overestimated precipitation as measured by CHIRPS, while it underestimated precipitation in October (as shown in Figure 11b), meaning earlier beginning and ending of the rainy season in Cabo Verde are simulated in the Coupled approach. Overall, the uncoupled simulation main challenge is the overestimation of monthly mean precipitation across all three subregions, especially during the rainy season, when it produced almost twice as much the precipitation observed by rain gauge and CHIRPS.

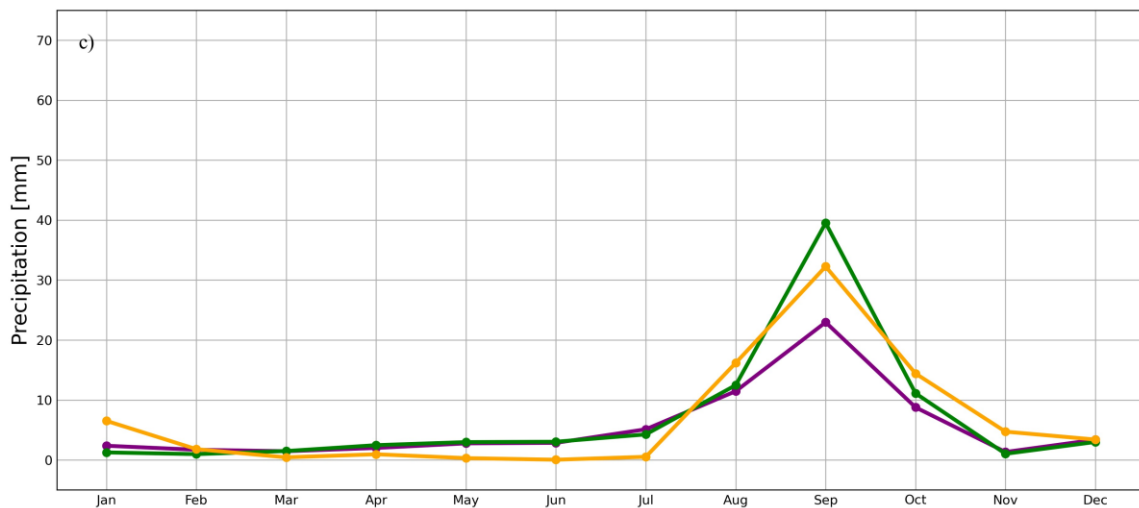
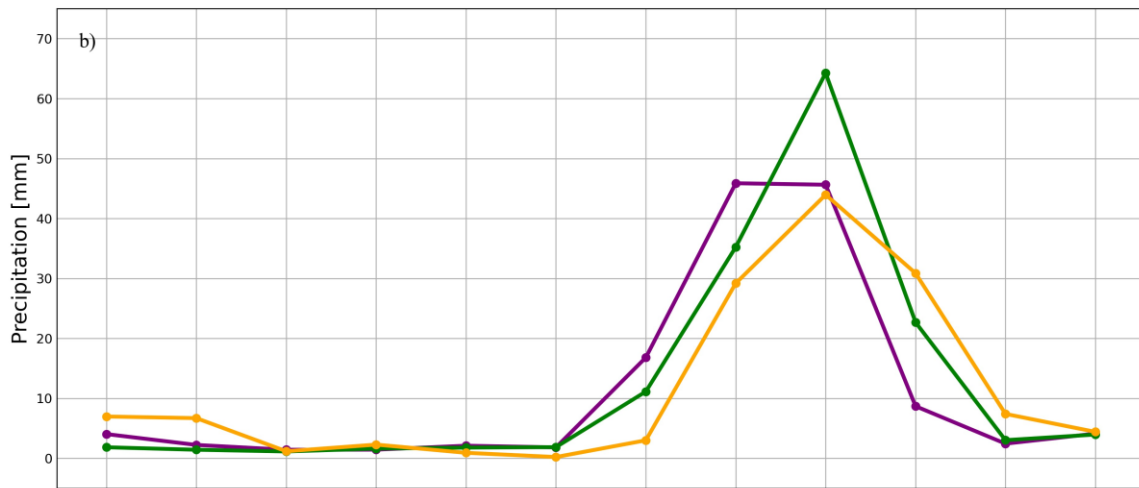
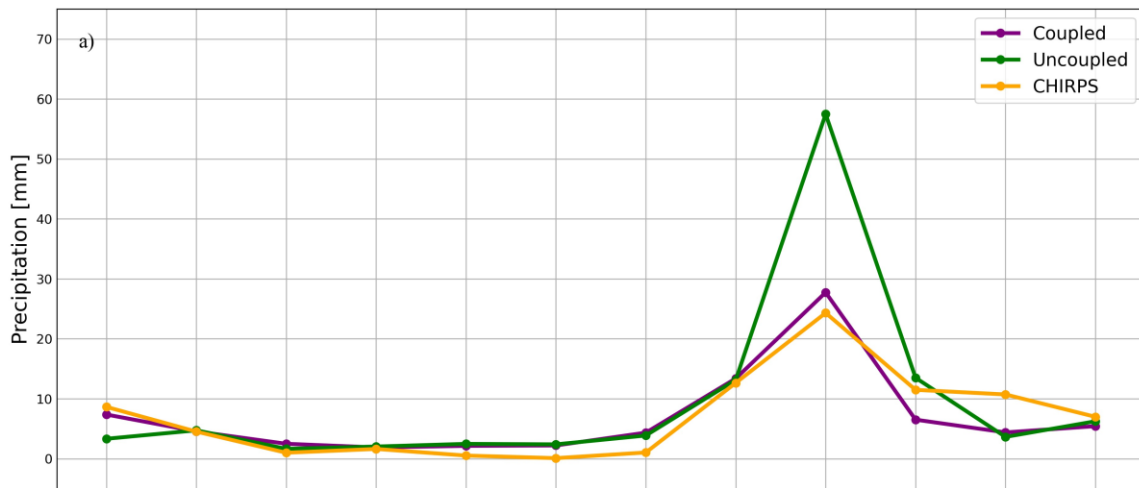


Figure 11: Monthly mean precipitation over Northern Islands (a), Southern Islands (b), Eastern Islands (c) for Coupled, Uncoupled, and CHIRPS for the period from 1981 to 2010.

4.2.2. Rainfall interannual variability

This section presents an analysis for the interannual variability of rainfall in Cabo Verde and sub-regions. Figure 12 shows the annual precipitation anomaly over Cabo Verde based on the four different data sources: rain gauge (low latitude), CHIRPS, Coupled and Uncoupled models. The anomaly is a deviation from the average value, so a positive anomaly indicates that the precipitation was higher than average, while a negative anomaly indicates that the precipitation was lower than average. The dashed black line represents a 5-years moving average, which smooths out short-term fluctuations and highlights longer-term trends. Rain gauge and CHIRPS, respectively figure 12a and 12b, are consistent in reproducing periods with similar signs, for instance the prevalence of negative anomalies during the first half of 1980's and 1990's, and the dominance of positive anomalies at the end of 2000's. The anomalies in rain gauge and CHIRPS varied between -50 to 100 mm per year. Rain gauge prevalence of negative anomalies from 1980's to the beginning of 1990's is consistent with the well established in the literature widespread lack of precipitation across the Sahel region. So is the irregular recovery of precipitation after 1990's seen in both rain gauge and CHIRPS. Models, both Coupled and Uncoupled (Figure 12c and 12d), do not seem to capture these features properly. During the 1980's, positive anomalies were prevalent in the uncoupled model, opposite to the observations. Coupled model showed some progress for this period by increasing the number of years with negative anomalies. However, for the 1990's first half, coupled simulations struggled to capture the features observed, producing strong deviation precipitation from average that reaches up to 150 mm per year. Although it is more difficult to point out a clear improvement due to coupled simulation for the interannual variability of precipitation over Cabo Verde, it is clear that atmosphere-coupling approach reshape rainfall variability at this and longer scale, which somehow is summarised in the moving average that provided insight into longer-term trends in precipitation over Cabo Verde.

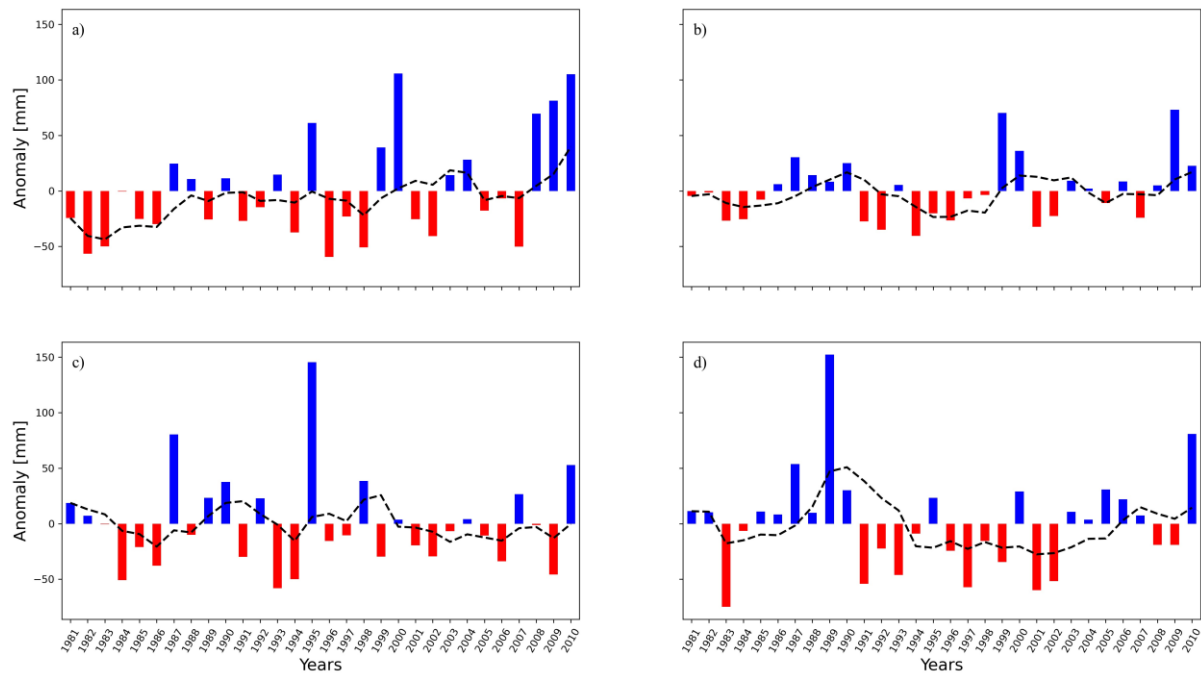


Figure 12: Annual precipitation anomaly over Cabo Verde based on rain gauge (a), CHIRPS (b), Coupled model (c) and Uncoupled model (d); It is also added a 5-years moving average (black dashed line). Anomalies are with respect to the annual mean precipitation calculated for the 1981–2010 period.

Figure 13 shows the annual precipitation anomalies over Northern Islands from 1981 to 2010. It is worth mentioning the signs mismatch between models and CHIRPS for this region. For the CHIRPS, positive anomalies persisted throughout the 1980's, even for 1981 when negative anomalies persisted in all other subregions and in Cabo Verde as a whole (Figure 12), and from 1990's on variability between periods of positive and negative values is seen. Coupled and Uncoupled simulations showed some similarity in their anomalies patterns, for instance the dominance of positive anomalies for the second half of 1980's, which in terms of sign is consistent with CHIRPS (positive), but with significant difference in magnitude. From 1990's onward, coupled and uncoupled simulated a prevalence of negative anomalies, especially the former modelling approach. In general, the 5 years moving average lines show some similarity between the models and observational dataset for the Northern region, the first 10 years with a prevalence of positive anomalies, and the remaining period with negative anomalies being dominant.

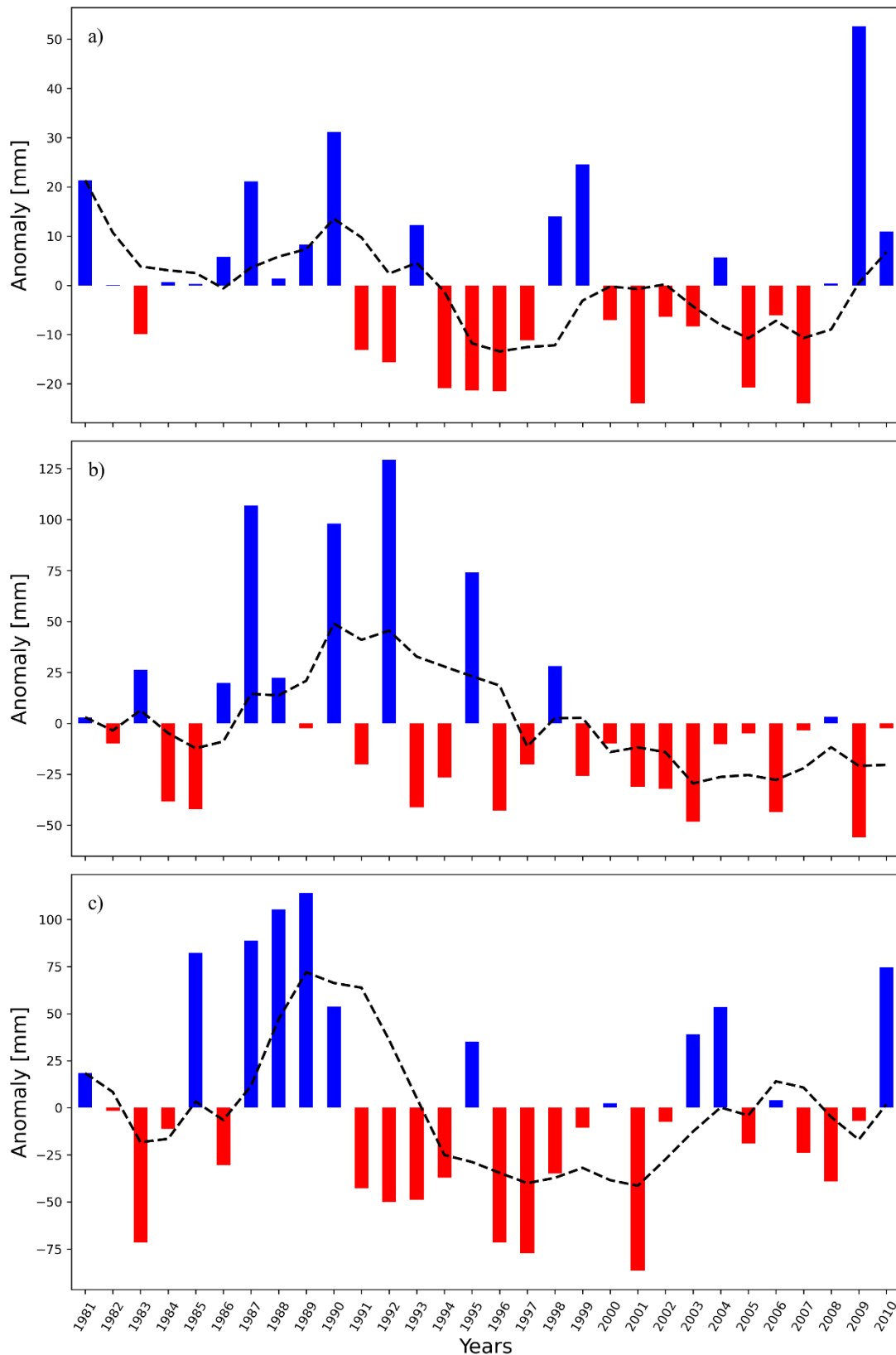


Figure 13: Annual precipitation anomaly over Northern Islands based on CHIRPS (a), Coupled model (b) and Uncoupled model (c): It is also added a 5-years moving average (black dashed line). Anomalies are with respect to the annual mean precipitation calculated for the 1981–2010 period.

The annual precipitation anomaly over Southern Islands is displayed in Figure 14. CHIRPS shows prevalence of negative anomalies during the first half of 1980's and positive anomalies only occurring for the period between 1985, 1986 and 1987. Therefore, a long period of negative anomaly until the end of 1990's, afterward an irregular recovery in precipitation is observed from 2000's on. The Coupled model was able to capture the observed main features until the first half of 1990's better than Uncoupled. In general, both models started 1980's with a dominance of negative anomalies, following CHIRPS, and they were able to also simulate the short-wet period of 1986/1987. However, after the end of 1990, the models followed different paths, uncoupled persisted in the dominance of negative anomalies until the first half of 2000's, while coupled simulated a more variable scenario.

Figure 15 presents the results for the annual anomaly over Eastern Islands, and shows different results between CHIRPS and the two model simulations. CHIRPS dataset exhibits the prevalence of negative anomalies throughout the 1980's and to some extent during the first half of 1990's. An irregular recovery of rainfall during the 2000's is seen, but with a period characterized by negative anomalies in the middle of 2000's. The most important difference identified between models and observation for the Eastern Islands is related to the prevalence of strong positive anomalies during the 1980's, especially for uncoupled model, a feature unseen in observational products and also for the previous sub-regions. Both simulations also simulate a persistent dominance of negative anomalies throughout 1990's and 2000's, which is not supported by observation. This behavior led to the distinct trends observed for the 5-years moving average between model and observational datasets. At this point it is worth mentioning that Eastern islands are the driest among Cabo Verde islands, their annual rainfall is usually explained by a couple of passing by precipitation systems during the rainy season, which can be a real challenge for models to reproduce its rainfall features.

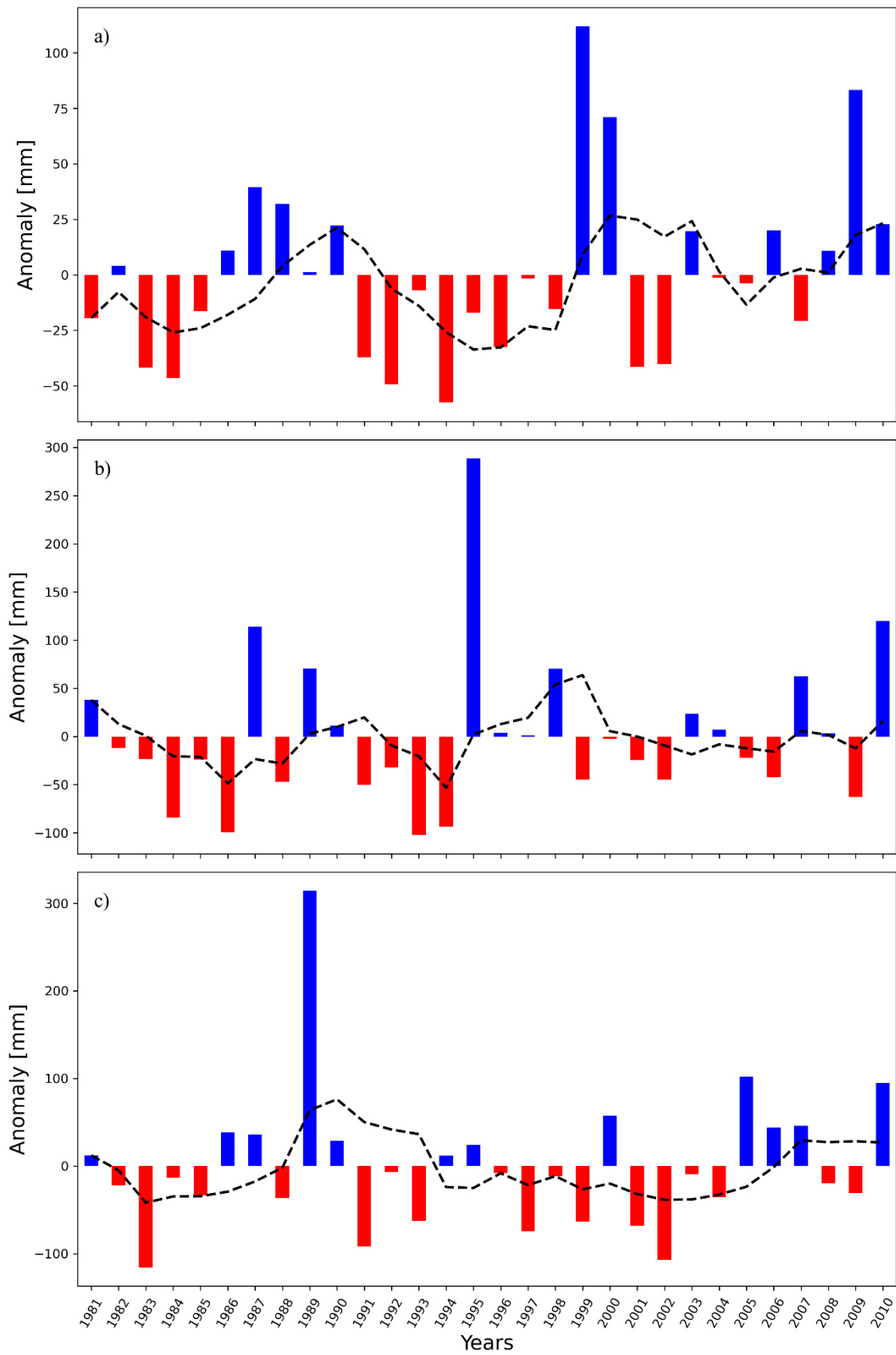


Figure 14: Annual precipitation anomaly over Southern Islands based on CHIRPS (a), Coupled model (b) and Uncoupled model (c): It is also added a 5-years moving average (black dashed line). Anomalies are with respect to the annual mean precipitation calculated for the 1981–2010 period.

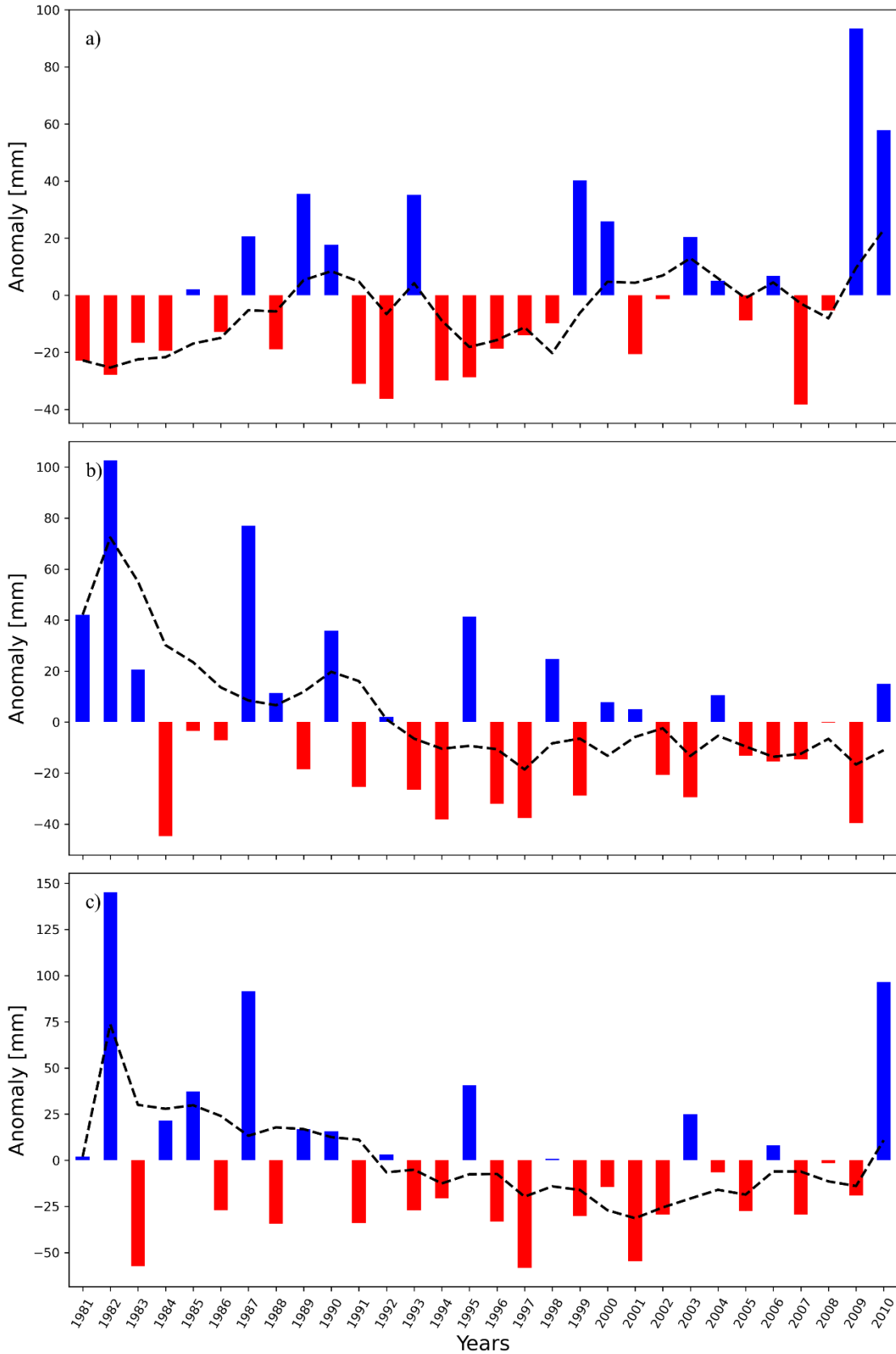


Figure 15: Annual precipitation anomaly over Eastern Islands based on CHIRPS (a), Coupled model (b) and Uncoupled model (c): It is also added a 5-years moving average (black dashed line). Anomalies are with respect to the annual mean precipitation calculated for the 1981–2010 period.

4.2.3. Long term drought assessment

In this section, results from Standardized Precipitation Index (SPI) application to assess and evaluate coupled and uncoupled models' ability to simulate long-term climatological drought in Cabo Verde and for the three subregions. According to Ferreira, (2020), droughts are the main drivers of macro-economic impact for the country with relevant local economic impact. Since the focus is on hydrological droughts, for the analysis the SPI-36 months' time scale was selected. The following SPI analysis focus on very wet events (SPI values between 1.5 to 1.99); extremely wet event (SPI values higher than +2.0); very dry events (SPI values between -1.5 to -1.99); and extremely dry events (SPI values lower than -2), these are the events expected to have the largest social, economic and environmental negative consequences. Figure 16 compares SPI-36 evolution for CHIRPS, and the two modelling approaches, coupled and uncoupled, for the Cabo Verde entire domain. The results show significant agreement between the CHIRPS and coupled (Figure 16a and Figure 16b) during the 1980's and the first half of 1990's, revealing consistency of these coupled to feature long term dry and wet conditions in Cabo Verde, at least for the period mentioned. CHIRPS datasets show a relatively long period of dry tendency from 1984 to 1987, although pronounced, but aligned with the Sahel region's profound drought experienced during the 1980's (Diawara et al., 2016). From the previous anomalies analysis and literature (Ferreira, 2020), this first drought event started well before, at least from 1981 and peaked around 1984. As coupled simulations reveal, this drought event was followed by a relatively long-wet period in Cabo Verde, from 1988 to 1993, consistent with the positive anomalies of precipitation in the previous years, and which is not seen in the Sahel rainfall time series (Diawara et al., 2016), The Sahel region experienced a short period of positive anomalies in its precipitation in 1988. There was then a return to dry conditions in Cabo Verde from 1993 to 1996 in the CHIRPS dataset. This long-term drought in 1990's, mainly in 1992 and 1998, caused disruptions such as food shortages affecting thousands of people in Cabo Verde (Ferreira, 2020). However, despite a few periods of normal and minor dry events from 2000 to 2010 rainfall, Cabo Verde experienced a recovery in its rainfall, which also led to some flood events (Ferreira, 2020).

Coupled and uncoupled simulations did not show a similar pattern throughout the entire time period (Figure 16c and 16d), which revealed that ocean-atmosphere coupling does produce substantially different results for precipitation over the Cabo Verde region. Despite a short-wet scenario at the beginning of the coupled run, both simulations seem to capture the sign of a drought event in the middle of 1980's. Coupled produced a better capture of its

severity. The wet conditions from the end of 1980's to the beginning of 1990's observed in Cabo Verde were also identified by the models, however with distinct severity. From 1988 to 1993, the coupled SPI indicated normal and wet periods, but uncoupled SPI was mostly normal periods. In the coupled run the wet conditions peaked from 1997 to 1998, while the uncoupled model kept SPI between -1 to 1 from 1987 until 1998, producing a much longer normal scenario. From the beginning of 2000's to the end, the transition for a normal period present in the observation was captured by coupled simulation. However, while the coupled run was not able to reproduce its magnitude properly, for the Uncoupled run, from 1999 to 2010, there was a succession of dry and wet conditions, with prevalence of wetness extending throughout the 2000's, while the last more significant wet condition in observation was registered in 1990's.

In summary, from the beginning of the time series, over Cabo Verde CHIRPS and coupled model showed good agreement until 1995, when occurred a transition to the 1990's dry and wet conditions. After that, there are relevant mismatches between observations and models and also between the models.

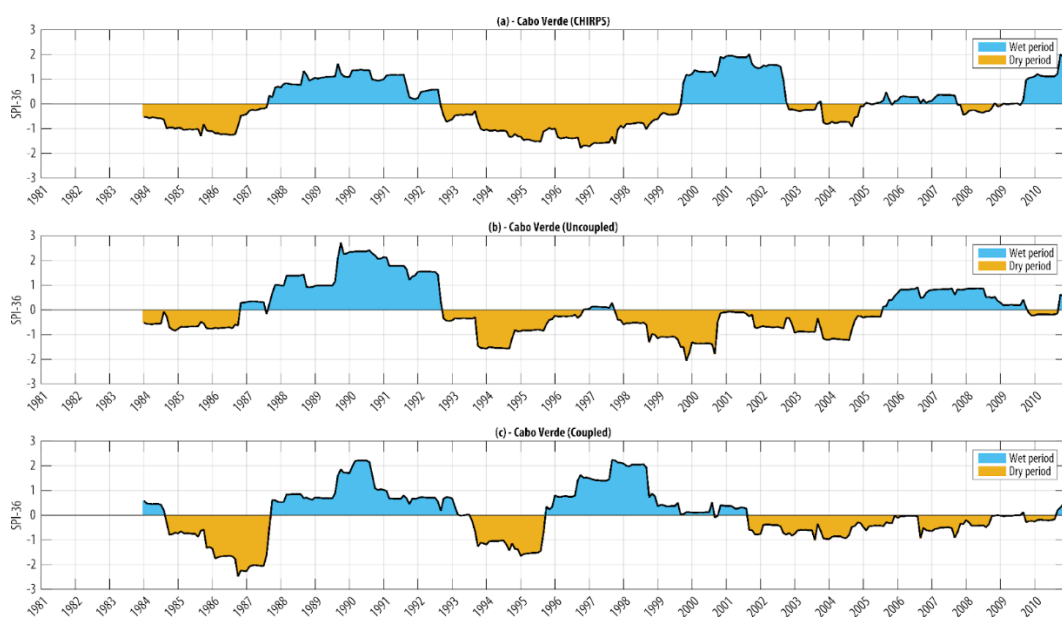


Figure 16: Standard Precipitation Index 36-month calculated for Cabo Verde based on: CHIRPS (b), Coupled model (c) and Uncoupled model (d) datasets from 1981 to 2010.

For the Northern Islands, the 36-months SPI results show some differences between CHIRPS and the coupled and uncoupled models at the beginning of 1980's (Figure 17a and 17b). While the CHIRPS started with a normal period from 1984 to 1987, coupled started with dry to normal conditions, which persisted until 1988, and then was followed by a wet period. From 1988 to 1993, similar features were observed between the three datasets, a prevalence of

wet conditions. After 1993, the coupled model persisted the wet tendency while the uncoupled change to dry tendency as the observation indicates. Eventually, the coupled run shifted to normal to dry conditions from 1996 on. Uncoupled features show a long dry tendency period that extended from 1993 until 2000's. This is not consistent with CHIRPS which shows a wet period between 2000 and 2002. From 1996 to 2010, the uncoupled model was characterized by normal conditions, but inverted signs when compared with CHIRPS. Instead of a dry period in the middle of wet scenarios, as seen in CHIRPS, the uncoupled run was characterized by a wet period (2005 - 2007) in between two dry scenarios.

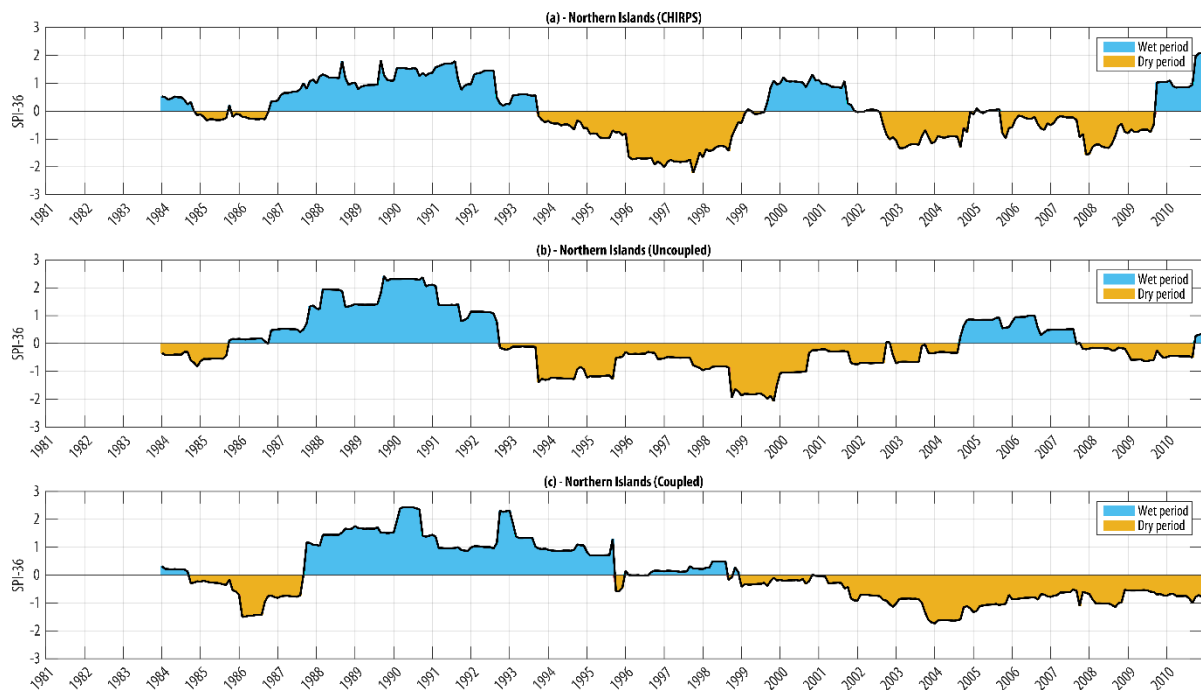


Figure 17: Standard Precipitation Index 36-month calculated for Northern Islands based on: CHIRPS (a), Coupled model (b) and Uncoupled model (c) datasets.

For the Southern Islands, CHIRPS and models presented better agreement from 1984 to 1996 in the succession of dry and wet periods than for Northern Island, as shown in Figure 18a, 18b and 18c. They both coupled and uncoupled runs simulate the transition from dry to a wet scenario although there are differences in the magnitude and time. From 1996 to 2010 there was a mismatch between CHIRPS and models. CHIRPS show a dry scenario from 1996 to 1999 followed by a wet period from 2000 to 2003, then follow normal or near normal conditions until 2010. The coupled and uncoupled (Figure 18b and Figure 18c) dataset began by reflecting more or less similarity for the period of 1984 - 1995, and from 1996 on substantial differences between them started to appear. The coupled simulation presents a sharp shift from

dry scenario to wet condition during 1996, only seen in the observation from 1999 to 2000. From 1996, the uncoupled persisted with normal to dry conditions until 2005.

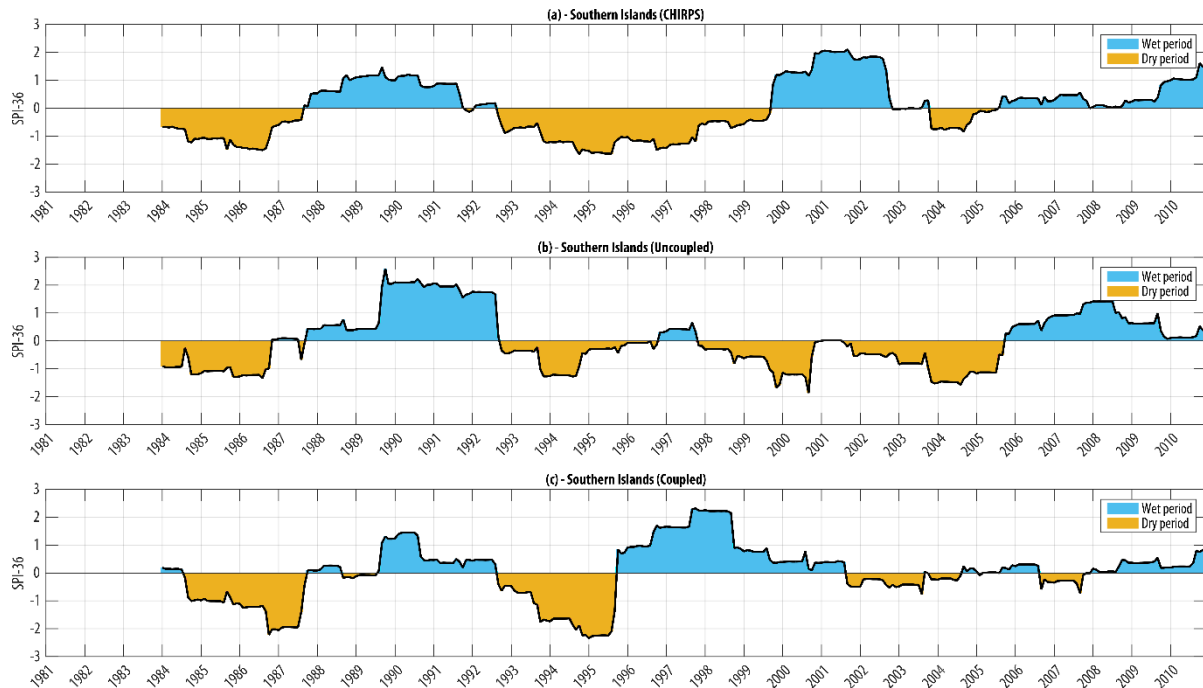


Figure 18: Standard Precipitation Index 36-month calculated for Southern Islands based on: CHIRPS (a), Coupled model (b) and Uncoupled model (c) datasets.

The results in Figure 19 show the 36 months-SPI evolution from CHIRPS, coupled and uncoupled simulations for the Eastern Islands. The results suggest a certain level of agreement between the CHIRPS and models (Figure 19a, 19b and 19c), mainly from 1987 to 1997, but it is possible to identify relevant differences. The dry period identified in CHIRPS from 1997 to 2003 was not captured by the models. Normal conditions were simulated by the coupled run and wet scenario by the uncoupled simulation at this period. However, it is possible to see that the coupled and uncoupled models were not able to reproduce well the conditions observed from 1987 to the beginning of the 2000's, but coupled was unable to reproduce the normal condition period between 2003 to 2009, which uncoupled run reproduces.

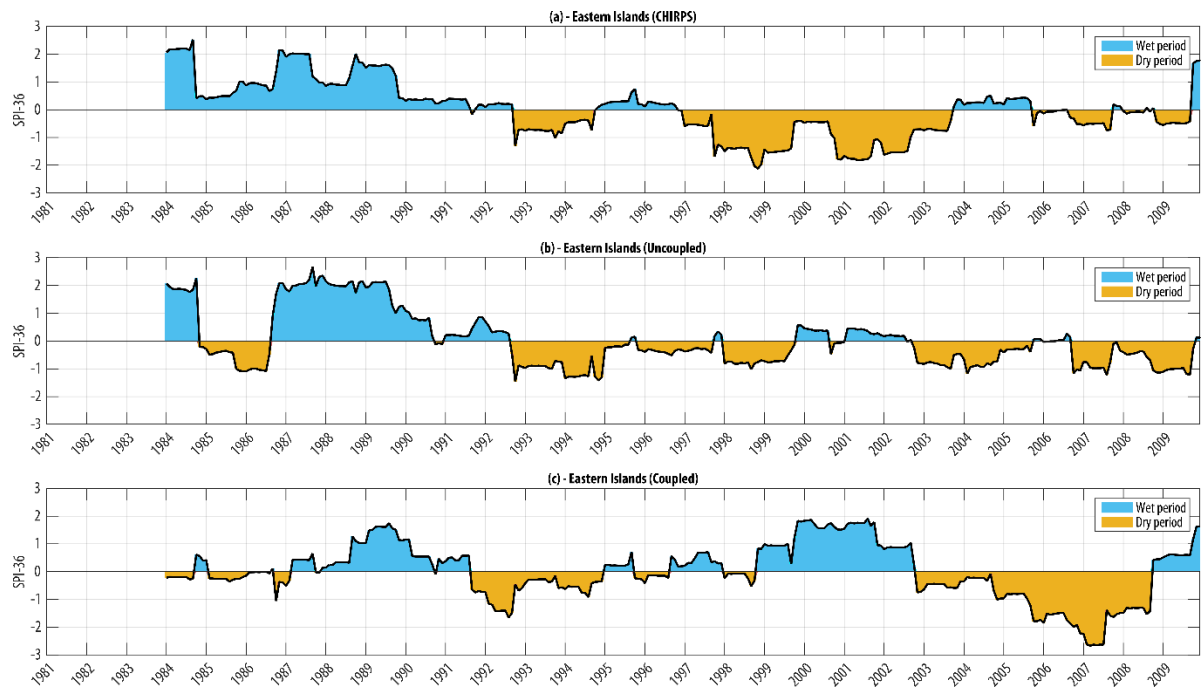


Figure 19: Standard Precipitation Index 36-month calculated for Eastern Islands based on: CHIRPS (a), Coupled model (b) and Uncoupled model (c) datasets.

4.3. Added value of seasonal mean monthly precipitation

The current study has been focused on the evaluation of the potential benefits of simulating rainfall climatological features over the Cabo Verde islands by applying a regionally coupled atmosphere-ocean model. The added value (AV) metric was calculated for each grid box using Equation 1. The simulated precipitation by REMO (uncoupled) and ROM (coupled) modelling systems was compared to the CHIRPS rainfall, used as observational reference.

Figure 20 describes the Added Value (AV) of simulating seasonal precipitation for West Africa using the coupled model (ROM) compared to the uncoupled model (REMO). Positive (negative) values indicate a lower (higher) precipitation bias of ROM compared to REMO. Focusing on the months that enclose the West Africa rainy season (JJASO), the results show that the bias in ROM for JJA is increased mainly over the Sahel western region and Gulf of Guinea countries. Yet in JJA, over the coastal region of Guinea and Sierra Leone ROM bias is decreased. For SON, there is a decrease in ROM bias for Senegal and Guinea coast, and inland mainly over the eastern Sahel. The results for West Africa did not show a strong generalized added value during the rainy season. A tendency to bias increase for ROM is observed in JJA, which is reverted to a lower bias for ROM during SON when compared with REMO. This is consistent with the differences obtained between CHIRPS and the two simulations (Figure 6). During JJA both overestimated precipitation over West Africa, but coupled produced higher

overestimation. For SON it was the opposite, the uncoupled produced the higher overestimation.

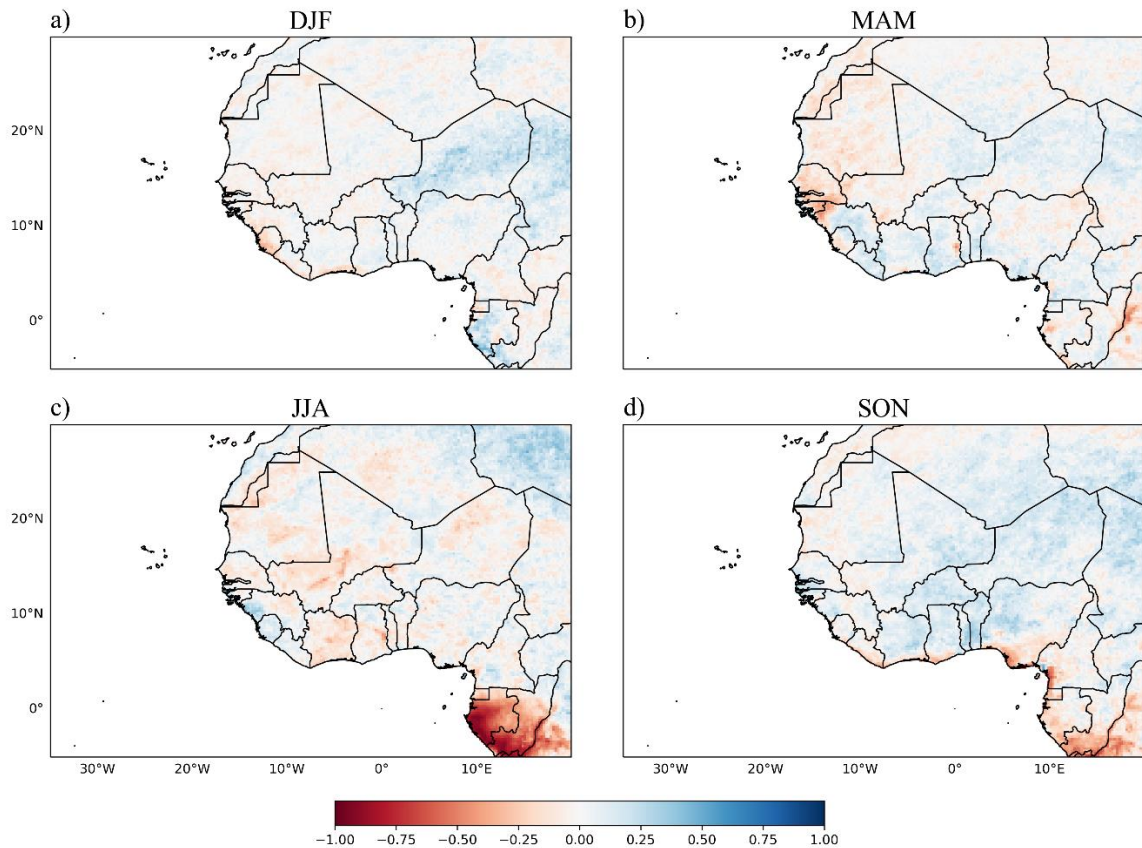


Figure 20: Added value AV of seasonal mean monthly precipitation for West Africa in ROM compared to REMO. Reference dataset is CHIRPS from 1981 to 2010 for December to February (DJF) (a), March to May (MAM) (b), July to August (JJA) (c) and September to November (SON) (d). Positive (negative) values indicate a lower (higher) precipitation bias of ROM compared to REMO.

Figure 21 shows the added value results for seasonal precipitation over Cabo Verde. The patterns of precipitation bias vary from season to season and AVs magnitudes are not substantially high. In DJF, the precipitation bias in ROM is reduced all over the country, however it is necessary to point out that this is the dry season. For MAM, which is still part of the dry season, bias reduction for ROM is observed in some of the Islands. In JJA, when the rainy season starts, there is an increase in ROM precipitation bias over the island of Santo Antão, Santiago and Fogo, exactly those with rugged topography. In JJA ROM overestimation of precipitation was higher than that of REMO, in particular for the southern portion of the country. Furthermore, ROM precipitation bias decreases all over the country in SON, with ROM presenting a better simulation of rainfall during the rainy season peak in September.

The results of added values for ASO (August-September-October), the period that accounts for almost 60% of the annual rainfall, is displayed in Figure 22 and also shows that there is reduction in ROM precipitation bias during these months. Although added values are still not very high, this is a benefit worth emphasizing, ROM's ability to improve the simulation of the amount of rainfall during the Cabo Verde rainy season and throughout the country.

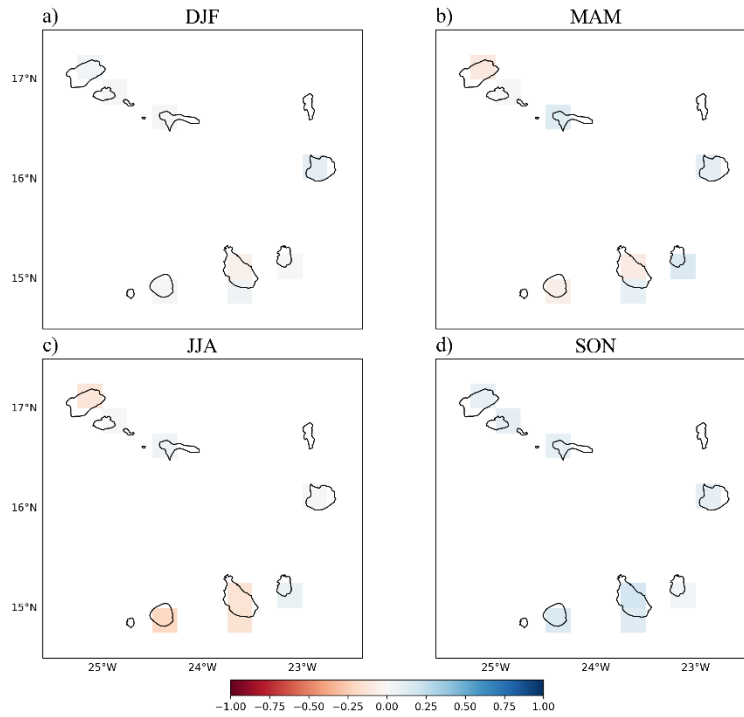


Figure 21: Added value AV of seasonal mean monthly precipitation for Cabo Verde in ROM compared to REMO. Reference data set is CHIRPS from 1981 to 2010 for December to February (DJF) (a), March to May (MAM) (b), July to August (JJA) (c) and September to November (SON) (d). Positive (negative) values indicate a lower (higher) precipitation bias of ROM compared to REMO.

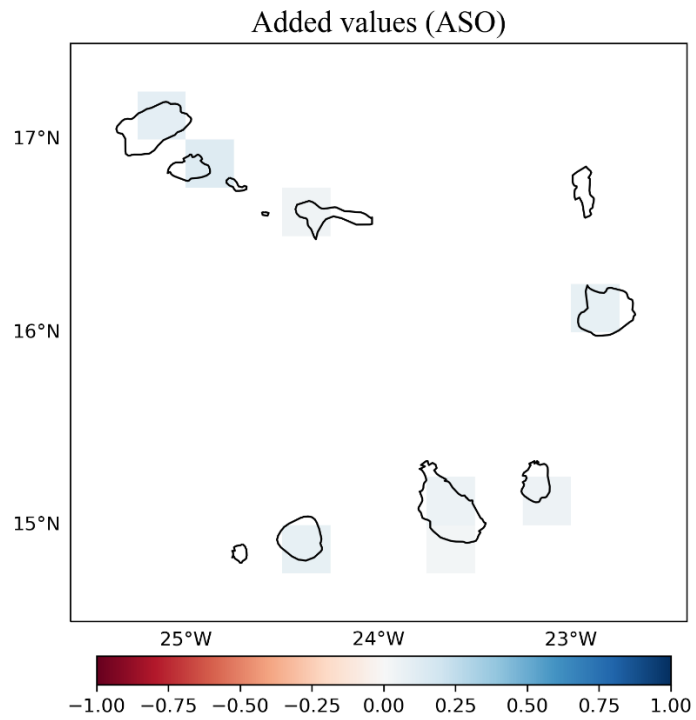


Figure 22: Added value AV of seasonal mean monthly precipitation for West Africa in ROM compared to REMO. Reference data set is CHIRPS from 1981 to 2010 for August September and October (ASO).

5. Discussion

The present study compares seasonal and spatial precipitation features across Cabo Verde islands simulated by a regional atmosphere-ocean coupling system (ROM) against the simulation performed by an uncoupled model (REMO). The main hypothesis is that West Africa, particularly the offshore islands, has a precipitation regime strongly connected to atmosphere-ocean interactions. That coupled model can improve these interactions and precipitation patterns (Weber et al., 2022).

In general, the two models' approaches were able to simulate the major seasonal and spatial features of precipitation across West Africa and also over Cabo Verde archipelago. The months from December to April, which constitute the dry season in West Africa, have less than 50 mm/month. During this season, north-easterly winds, known as the Harmattan winds blow across the Sahara Desert down south and to the eastern tropical Atlantic (Barua et al., 2020) bringing dry and dusty air mass. In addition, this period's inter-tropical convergence zone (ITCZ) is further south. During the months from May to June, the rainfall frequency and intensity increase, and this marks the beginning ITCZ northward march and of the rainy season in West Africa. This transition timing was also well represented by the models. By late July, rainfall becomes more frequent marking a mature stage of the West African summer monsoon season (Eric et al., 2020 and Sultan & Gaetani, 2016). This is when both models simulate their highest precipitation amount across West Africa. However, during JJA, both coupled and uncoupled overestimated the observed rainfall across continental region of West Africa, with coupled presenting slightly higher overestimation across inland regions and lower overestimation along some coastal regions. This suggests that the regional coupled atmosphere-ocean model simulates the Inter Tropical Convergence Zone (ITCZ) shifted further north than in the uncoupled model REMO. Similar findings, forcing ROM and REMO with the climate global model MPI-ESM-LR, were reported by Weber et al., (2022), who suggested that this shift could be due to colder sea surface temperatures in Gulf of Guinea simulated by ROM and increased sea-level pressure, which force ITCZ position northward. Regarding the ability of coupled models to reduce the bias in precipitation along some coastal region of West Africa, it was also observed by Paxian et al., (2016), who found a reduced precipitation bias in decadal climate predictions for the Guinea Coast with regionally coupled atmosphere–ocean model.

Another point to highlight during JJA is that over the ocean and at the south of Cabo Verde, uncoupled simulates a much stronger and narrower ITCZ rainbelt than coupled. This feature is also seen during SON, however, over continental areas of West Africa, at this time the coupled model produced less rain than the uncoupled model, the opposite when compared with the JJA period. Similar behaviour is also identified over Cabo Verde Island, which lead to a higher rainfall overestimation for uncoupled over the archipelago at the peak of the country's rainy season. A result that revealed higher consistency with the observations. Furthermore, it has been shown by Haensler et al., (2011) and Weber et al., (2022) that the application of a bias-corrected SST leads to improved precipitation results in regional climate models over southern Africa.

Rainfall season over Cabo Verde Island reaches its peak later on in September, when ITCZ reaches its most northward position, especially in the Southern Islands, where precipitation with intensity up to 100 mm/month is observed. Not all islands are significantly affected by ITCZ displacement, the southern islands certainly are, mainly those characterised by high topography. This is why some areas have on average rainfall at least twice or three times as low as other regions, within the rainy season. In October and November, rainfall varies between 30 and 50 mm/month, which shows the ending of the rainy season and the beginning of the main dry season in Cabo Verde. Coupled simulation of monthly mean precipitation provided a better representation of Cabo Verde's total seasonal precipitation compared to the uncoupled simulation. This is mainly due to the coupled model's ability to better reproduce the peak of precipitation, since it overestimates and underestimates precipitation at the beginning (August) and ending (October) of the rainy season in the archipelago. Furthermore, the ocean-atmosphere coupled model results for each defined subregion show improvements in the simulation of the seasonal cycle and spatial distribution of precipitation across the group of islands. However, an important aspect to highlight is that none of the models were able to reproduce precipitation amounts when considering the high-altitude rain gauge stations. Previous studies have discussed and highlighted the limitations of not considering higher spatial resolution in simulating small islands with complex topography (Carrillo et al., 2023).

For the interannual variability of anomalies, in general, the coupled model performed better for the entire country and for the southern islands, and both models did not perform for the northern and eastern islands as good as they perform for the Southern islands. For the long-term drought, somehow both models managed to simulate consistently the alternation of dry and wet conditions between the 1980's and 1990's for Cabo Verde and for the southern islands

(Ferreira, 2020), but afterward they lacked consistency among them and between them and the observation. The signals of Sahel historical drought during 1980's and the irregular recovery of regional rainfall after 1990's (Held et al., 2005) were somehow seen in all the dataset, including both models. But as identified in the observational reference dataset, some relevant differences were also observed, such as the wet period in the at the end of 1980's and beginning of 1990's, which may be explained by Cabo Verde Island oceanic conditions.

Another interesting aspect is that for the simulations and observation, differences in climate events (dry and wet) intensity, duration and even signal were identified between the sub-regions, despite the relatively small spatial scale. Which reveals that despite Cabo Verde's small domain, the northern region and southern region can experience even opposite climate conditions in terms of rainfall, a scenario well documented by (Ferreira, 2020) .

As highlighted by Weber et al., (2022), evaluating the effectiveness of a regionally coupled atmosphere-ocean model over small islands is challenging due to the limited availability of reference data. The CHIRPS precipitation dataset is the only source of gridded precipitation information over Cabo Verde, with a spatial resolution of 0.25° (approximately 28 km). Nevertheless, the results of the present study indicate that the regionally coupled atmosphere-ocean model (ROM) improves the seasonal cycle and spatial distribution of rainfall over Cabo Verde by mainly reducing the precipitation bias observed in uncoupled model during the rainy season months (ASO) in Cabo Verde. As a consequence, positive Added Value was found over all islands during the rainy season, confirming, therefore, Weber et al., (2022) results that the regionally coupled atmosphere–ocean model ROM can reduce the precipitation bias over the islands offshore the African continent compared to the atmosphere-only model REMO.

6. Conclusions

Simulating precipitation characteristics over small island states using global climate models does not provide specific and realistic information. This is due to the fact that precipitation formation in the small islands is influenced by various factors associated with regional and local scales, including the sea surface temperature of nearby oceans, evaporation, moisture transport, regional meteorological phenomena and very often, rugged topography. Therefore, regional downscaling of the global climate model and integrating atmosphere-ocean interactions can be the first two important steps to improve precipitation representation for small island states, especially those in tropical regions. In this study, we evaluated the benefits of using a regional atmosphere-ocean coupling system to simulate historical precipitation over the Cabo Verde archipelago, in the eastern Atlantic Ocean located off the coast of Western Africa.

Our results showed that, compared to an uncoupled model, the coupled model simulates the annual precipitation cycles over Cabo Verde more accurately and produces more realistic precipitation amounts across the country, as confirmed by comparison with observational data. Consequently, positive AV was found over all islands during the rainy season. The coupled model generally outperformed the uncoupled model in terms of interannual variability of precipitation over Cabo Verde and its subregions. For the long-term drought, although the coupled model managed to simulate consistently the alternation of dry and wet conditions between the 1980's and 1990's for Cabo Verde and the southern islands, we did not see a clear superior performance when compared with the uncoupled model. After 1990's both models lacked consistency among them and against observation. This suggests sensitivity of the models to large scale climate mode background.

In summary, the results of the present study suggest that there are benefits in using a coupled atmosphere-ocean model to simulate precipitation over Cabo Verde islands. This finding is important because regional climate change analyses and projections are typically based on uncoupled regional climate models. It is important to note that our results have some limitations regarding their validity. Factors such as the spatial resolution, which is not entirely adequate to simulate complex topography, and model domain can affect precipitation results. Observational datasets and their management are also a challenge. The CHIRPS resolution cannot capture all the complex structure of precipitation posed by the complex topography of the country. The available rain gauge station number is biased to areas where topography

strongly affects rainfall, therefore unsuitable to promote a fair evaluation of the regional models analyzed. To minimize some of these challenges, some recommendations are provided as follows.

7. Recommendations

- A regionally coupled atmosphere-ocean climate model can improve the simulation of precipitation characteristics in Cabo Verde. Therefore, for further research, we recommend continuity in exploring regionally coupled atmosphere-ocean models for simulating precipitation over Cabo Verde and other African regions. The analysis of the long-term drought highlighted an important aspect: the performance of the models under different large-scale climate mode variability.
- It is fundamental to investigate the benefit of using a regionally coupled atmosphere-ocean with spatial resolution tailored to properly represent the topography of Cabo Verde islands. Our results showed that none of the models did not capture precipitation across rugged topography well.
- Extend the current historical investigation of the influence of ocean-atmosphere interaction on the temperature variable.
- Considering the benefits obtained in simulating Cabo Verde historical rainfall using a coupled model, future studies are recommended to investigate the impact of this approach on the future climate projections of precipitation over Cabo Verde Island. This study shows that long-term drought occurrence varied between coupled and uncoupled, since the coupled provide a more physically consistent approach, this can benefit future projections.

8. References

- Abatan, A. A., Gutowski, W. J., Ammann, C. M., Kaatz, L., Brown, B. G., Buja, L., Bullock, R., Fowler, T., Gilleland, E., & Gotway, J. H. (2017). Multiyear droughts and pluvials over the upper Colorado River basin and associated circulations. *Journal of Hydrometeorology*, 18(3), 799–818. <https://doi.org/10.1175/JHM-D-16-0125.1>
- Akinsanola, A. A., Ajayi, V. O., Adejare, A. T., Adeyeri, O. E., Gbode, I. E., Ogunjobi, K. O., Nikulin, G., & Abolude, A. T. (2018). Evaluation of rainfall simulations over West Africa in dynamically downscaled CMIP5 global circulation models. *Theoretical and Applied Climatology*, 132(1–2), 437–450. <https://doi.org/10.1007/s00704-017-2087-8>
- Barua, S., Newth, D., & Valenzuela, E. (2020). Does Climate Variability Affect Agricultural Trade? *SSRN Electronic Journal*, 1–38. <https://doi.org/10.2139/ssrn.3680390>
- Cabos, W., de la Vara, A., Álvarez-García, F. J., Sánchez, E., Sieck, K., Pérez-Sanz, J. I., Limareva, N., & Sein, D. V. (2020). Impact of ocean-atmosphere coupling on regional climate: the Iberian Peninsula case. *Climate Dynamics*, 54(9–10), 4441–4467. <https://doi.org/10.1007/s00382-020-05238-x>
- Cabos, W., Sein, D. V., Durán-Quesada, A., Liguori, G., Koldunov, N. V., Martínez-López, B., Alvarez, F., Sieck, K., Limareva, N., & Pinto, J. G. (2018). Dynamical downscaling of historical climate over CORDEX Central America domain with a regionally coupled atmosphere–ocean model. *Climate Dynamics*, 52(7–8), 4305–4328. <https://doi.org/10.1007/s00382-018-4381-2>
- Carrillo, J., Hernández-Barrera, S., Expósito, F. J., Díaz, J. P., González, A., & Pérez, J. C. (2023). The uneven impact of climate change on drought with elevation in the Canary Islands. *Npj Climate and Atmospheric Science*, 6(1), 1–11. <https://doi.org/10.1038/s41612-023-00358-7>
- Christensen, J. H., & Christensen, O. B. (2007). A summary of the PRUDENCE model projections of changes in European climate by the end of this century. *Climatic Change*, 81(SUPPL. 1), 7–30. <https://doi.org/10.1007/s10584-006-9210-7>
- Di Luca, A., de Elía, R., & Laprise, R. (2012). Potential for added value in precipitation simulated by high-resolution nested Regional Climate Models and observations. *Climate Dynamics*, 38(5–6), 1229–1247. <https://doi.org/10.1007/s00382-011-1068-3>
- Diawara, A., Tachibana, Y., Oshima, K., Nishikawa, H., & Ando, Y. (2016). Synchrony of

- trend shifts in Sahel boreal summer rainfall and global oceanic evaporation, 1950–2012. *Hydrology and Earth System Sciences*, 20(9), 3789–3798. <https://doi.org/10.5194/hess-20-3789-2016>
- Dosio, A., Panitz, H. J., Schubert-Frisius, M., & Lüthi, D. (2015). Dynamical downscaling of CMIP5 global circulation models over CORDEX-Africa with COSMO-CLM: evaluation over the present climate and analysis of the added value. *Climate Dynamics*, 44(9–10), 2637–2661. <https://doi.org/10.1007/s00382-014-2262-x>
- Eric, E., Wandjie, B. B. S., Lenouo, A., Monkam, D., & Manatsa, D. (2020). African summer monsoon active and break spells cloud properties: Insight from CloudSat-CALIPSO. *Atmospheric Research*, 237, 104842. <https://doi.org/10.1016/j.atmosres.2020.104842>
- Fan, L., Chen, D., Fu, C., & Yan, Z. (2013). Statistical downscaling of summer temperature extremes in northern China. *Advances in Atmospheric Sciences*, 30(4), 1085–1095. <https://doi.org/10.1007/s00376-012-2057-0>
- Ferdinand, B. (2021). *Coastal View: Application of UAV in monitoring and mapping coastal habitats over Sao Vicente, Cabo Verde*. 66.
- Ferreira, G. (2020). Revisiting disasters in Cabo Verde : a historical review of droughts and food insecurity events to enable future climate resilience. *Revista Española de Estudios Agrosociales y Pesqueros (REEAP)*, 2020, 47–76.
- Fowler, H. J., Blenkinsop, S., & Tebaldi, C. (2008). The impact of the positive Indian Ocean dipole on Zimbabwe droughts Tropical climate is understood to be dominated by. *International Journal of Climatology*, 2029(March 2008), 2011–2029. <https://doi.org/10.1002/joc>
- Fuhrer, J., Smith, P., & Gobiet, A. (2014). Implications of climate change scenarios for agriculture in alpine regions - A case study in the Swiss Rhone catchment. *Science of the Total Environment*, 493, 1232–1241. <https://doi.org/10.1016/j.scitotenv.2013.06.038>
- Gao, X., Pal, J. S., & Giorgi, F. (2006). Projected changes in mean and extreme precipitation over the Mediterranean region from a high resolution double nested RCM simulation. *Geophysical Research Letters*, 33(3), 2–5. <https://doi.org/10.1029/2005GL024954>
- Gbobaniyi, E., Sarr, A., Sylla, M. B., Diallo, I., Lennard, C., Dosio, A., Dhiédiou, A., Kamga, A., Klutse, N. A. B., Hewitson, B., Nikulin, G., & Lamptey, B. (2014). Climatology, annual cycle and interannual variability of precipitation and temperature in CORDEX

- simulations over West Africa. *International Journal of Climatology*, 34(7), 2241–2257. <https://doi.org/10.1002/joc.3834>
- Giorgi, F. (2006). *Regional climate modeling: Status and perspectives*. 139, 101–118.
- Giorgi, F., Jones, C., & Asrar, G. (2009). Addressing climate information needs at the regional level: the CORDEX framework. ... *Organization (WMO) Bulletin*, 58(July), 175–183. http://www.euro-cordex.net/uploads/media/Download_01.pdf
- Government of Cabo Verde; Ministry of Environment and Rural Development. (2010). Second National Communication on Climate Change of Cabo Verde. *United Nations Framework Convention for Climate Change Ministry, October*, 1–162. <https://www.adaptation-undp.org/resources/assessments-and-background-documents/cape-verde-second-national-communication>
- Guenang, G. M., & Mkankam Kamga, F. (2014). Computation of the standardized precipitation index (SPI) and its use to assess drought occurrences in Cameroon over recent decades. *Journal of Applied Meteorology and Climatology*, 53(10), 2310–2324. <https://doi.org/10.1175/JAMC-D-14-0032.1>
- Guttman, N. B. (1998). Comparing the palmer drought index and the standardized precipitation index. *Journal of the American Water Resources Association*, 34(1), 113–121. <https://doi.org/10.1111/j.1752-1688.1998.tb05964.x>
- Haensler, A., Hagemann, S., & Jacob, D. (2011). Dynamical downscaling of ERA40 reanalysis data over southern Africa: Added value in the simulation of the seasonal rainfall characteristics. *International Journal of Climatology*, 31(15), 2338–2349. <https://doi.org/10.1002/joc.2242>
- Held, I. M., Delworth, T. L., Lu, J., Findell, K. L., & Knutson, T. R. (2005). *Simulation of Sahel drought in the 20th and 21st centuries*, by I. M. Held, T. L. Delworth, J. Lu, K. L. Findell, and T. R. Knutson, which appeared in issue 50, December 13, 2005, of. 103(50).
- IPCC. (2021). Linking Global to Regional Climate Change. In *Climate Change 2021 – The Physical Science Basis*. <https://doi.org/10.1017/9781009157896.012>
- Jacob, D. (2001). A note to the simulation of the annual and inter-annual variability of the water budget over the Baltic Sea drainage basin. *Meteorology and Atmospheric Physics*, 77(1–4), 61–73. <https://doi.org/10.1007/s007030170017>

- Jacob, D., Bärring, L., Christensen, O. B., Christensen, J. H., De Castro, M., Déqué, M., Giorgi, F., Hagemann, S., Hirschi, M., Jones, R., Kjellström, E., Lenderink, G., Rockel, B., Sánchez, E., Schär, C., Seneviratne, S. I., Somot, S., Van Ulden, A., & Van Den Hurk, B. (2007). An inter-comparison of regional climate models for Europe: Model performance in present-day climate. *Climatic Change*, *81*(SUPPL. 1), 31–52. <https://doi.org/10.1007/s10584-006-9213-4>
- Jacob, D., Elizalde, A., Haensler, A., Hagemann, S., Kumar, P., Podzun, R., Rechid, D., Remedio, A. R., Saeed, F., Sieck, K., Teichmann, C., & Wilhelm, C. (2012). Assessing the transferability of the regional climate model REMO to different coordinated regional climate downscaling experiment (CORDEX) regions. *Atmosphere*, *3*(1), 181–199. <https://doi.org/10.3390/atmos3010181>
- Jacob, D., Petersen, J., Eggert, B., Alias, A., Christensen, O. B., Bouwer, L. M., Braun, A., Colette, A., Déqué, M., Georgievski, G., Georgopoulou, E., Gobiet, A., Menut, L., Nikulin, G., Haensler, A., Hempelmann, N., Jones, C., Keuler, K., Kovats, S., ... Yiou, P. (2014). EURO-CORDEX: New high-resolution climate change projections for European impact research. *Regional Environmental Change*, *14*(2), 563–578. <https://doi.org/10.1007/s10113-013-0499-2>
- Jacob, D., Van Den Hurk, B. J. J. M., Andræ, U., Elgered, G., Fortelius, C., Graham, L. P., Jackson, S. D., Karstens, U., Köpken, C., Lindau, R., Podzun, R., Rockel, B., Rubel, F., Sass, B. H., Smith, R. N. B., & Yang, X. (2001). A comprehensive model inter-comparison study investigating the water budget during the BALTEX-PIDCAP period. *Meteorology and Atmospheric Physics*, *77*(1–4), 19–43. <https://doi.org/10.1007/s007030170015>
- Janicot, S., Caniaux, G., Chauvin, F., De Coëtlogon, G., Fontaine, B., Hall, N., Kiladis, G., Lafore, J. P., Lavaysse, C., Lavender, S. L., Leroux, S., Marteau, R., Mounier, F., Philippon, N., Roehrig, R., Sultan, B., & Taylor, C. M. (2011). Intraseasonal variability of the West African monsoon. *Atmospheric Science Letters*, *12*(1), 58–66. <https://doi.org/10.1002/asl.280>
- Jungclaus, J. H., Fischer, N., Haak, H., Lohmann, K., Marotzke, J., Matei, D., Mikolajewicz, U., Notz, D., & Von Storch, J. S. (2013). Characteristics of the ocean simulations in the Max Planck Institute Ocean Model (MPIOM) the ocean component of the MPI-Earth system model. *Journal of Advances in Modeling Earth Systems*, *5*(2), 422–446.

<https://doi.org/10.1002/jame.20023>

- Klutse, N. A. B., Sylla, M. B., Diallo, I., Sarr, A., Dosio, A., Diedhiou, A., Kamga, A., Lamptey, B., Ali, A., Gbobaniyi, E. O., Owusu, K., Lennard, C., Hewitson, B., Nikulin, G., Panitz, H. J., & Büchner, M. (2016). Daily characteristics of West African summer monsoon precipitation in CORDEX simulations. *Theoretical and Applied Climatology*, 123(1–2), 369–386. <https://doi.org/10.1007/s00704-014-1352-3>
- Kumar, P., Podzun, R., Hagemann, S., & Jacob, D. (2014). Impact of modified soil thermal characteristic on the simulated monsoon climate over south Asia. *Journal of Earth System Science*, 123(1), 151–160. <https://doi.org/10.1007/s12040-013-0381-0>
- Laing, A., & Evans, J. L. (2011). Introduction to Tropical Meteorology. *The COMET Program*, 8–10.
- Lewis, K., & C, B. (2016). “Climate Impacts in the Sahel and West Africa: The Role of Climate Science in Policy Making”, West African Papers,. *OECD Publishing, Paris*, 02. <https://doi.org/http://dx.doi.org/10.1787/5jlsmkwtjcd0-en>
- Lo, J. C.-F., Yang, Z.-L., & Pielke, R. A. (2008). Assessment of three dynamical climate downscaling methods using the Weather Research and Forecasting (WRF) model. *Journal of Geophysical Research*, 113(D9). <https://doi.org/10.1029/2007jd009216>
- Lucas-Picher, P., Christensen, J. H., Saeed, F., Kumar, P., Asharaf, S., Ahrens, B., Wiltshire, A. J., Jacob, D., & Hagemann, S. (2011). Can regional climate models represent the Indian monsoon? *Journal of Hydrometeorology*, 12(5), 849–868. <https://doi.org/10.1175/2011JHM1327.1>
- Mannaerts, C. M., & Gabriels, D. (2000). Rainfall erosivity in Cape Verde. *Soil and Tillage Research*, 55(3–4), 207–212. [https://doi.org/10.1016/S0167-1987\(00\)00104-5](https://doi.org/10.1016/S0167-1987(00)00104-5)
- Marsland, S. J., Haak, H., Jungclaus, J. H., Latif, M., & Röske, F. (2002). The Max-Planck-Institute global ocean/sea ice model with orthogonal curvilinear coordinates. *Ocean Modelling*, 5(2), 91–127. [https://doi.org/10.1016/S1463-5003\(02\)00015-X](https://doi.org/10.1016/S1463-5003(02)00015-X)
- Maurer, E. P., & Hidalgo, H. G. (2008). Utility of daily vs. monthly large-scale climate data: An intercomparison of two statistical downscaling methods. *Hydrology and Earth System Sciences*, 12(2), 551–563. <https://doi.org/10.5194/hess-12-551-2008>
- Mckee, T. B., Nolan J., D., & Kleist, J. (1993). THE RELATIONSHIP OF DROUGHT

- FREQUENCY AND DURATION TO TIME SCALES. *Journal of Surgical Oncology*, 105(8), 818–824. <https://doi.org/10.1002/jso.23002>
- Nandintsetseg, B., & Shinoda, M. (2013). Assessment of drought frequency, duration, and severity and its impact on pasture production in Mongolia. *Natural Hazards*, 66(2), 995–1008. <https://doi.org/10.1007/s11069-012-0527-4>
- Niederdrenk, A. L., Sein, D. V., & Mikolajewicz, U. (2016). Interannual variability of the Arctic freshwater cycle in the second half of the twentieth century in a regionally coupled climate model. *Climate Dynamics*, 47(12), 3883–3900. <https://doi.org/10.1007/s00382-016-3047-1>
- Nikulin, G., Jones, C., Giorgi, F., Asrar, G., Büchner, M., Cerezo-Mota, R., Christensen, O. B., Déqué, M., Fernandez, J., Hänsler, A., van Meijgaard, E., Samuelsson, P., Sylla, M. B., & Sushama, L. (2012). Precipitation climatology in an ensemble of CORDEX-Africa regional climate simulations. *Journal of Climate*, 25(18), 6057–6078. <https://doi.org/10.1175/JCLI-D-11-00375.1>
- Paeth, H., Born, K., Girmes, R., Podzun, R., & Jacob, D. (2009). Regional climate change in tropical and Northern Africa due to greenhouse forcing and land use changes. *Journal of Climate*, 22(1), 114–132. <https://doi.org/10.1175/2008JCLI2390.1>
- Parry, S., Wilby, L. R., Prudhomme, C., & Wood, J. P. (2016). A systematic assessment of drought termination in the United Kingdom. *Hydrology and Earth System Sciences*, 20(10), 4265–4281. <https://doi.org/10.5194/hess-20-4265-2016>
- Paxian, A., Sein, D., Panitz, H., Warscher, M., Breil, M., Engel, T., Tödter, J., Krause, A., Narvaez, W. D. C., Fink, A. H., Ahrens, B., Kunstmann, H., Jacob, D., & Paeth, H. (2016). *Journal of Geophysical Research : Atmospheres*. 1715–1735. <https://doi.org/10.1002/2015JD024143>.Received
- Rummukainen, M. (2010). State-of-the-art with regional. *Clim Change*, 1(1), 82–96. <https://doi.org/10.1002/wcc.008>
- Schoof, J. T. (2013). Statistical downscaling in climatology. *Geography Compass*, 7(4), 249–265. <https://doi.org/10.1111/gec3.12036>
- Sein, D. V., Koldunov, N. V., Pinto, J. G., & Cabos, W. (2014a). Sensitivity of simulated regional Arctic climate to the choice of coupled model domain. *Tellus, Series A: Dynamic Meteorology and Oceanography*, 66(1). <https://doi.org/10.3402/tellusa.v66.23966>

- Sein, D. V., Koldunov, N. V., Pinto, J. G., & Cabos, W. (2014b). Sensitivity of simulated regional Arctic climate to the choice of coupled model domain. *Tellus, Series A: Dynamic Meteorology and Oceanography*, 66(1), 1–18. <https://doi.org/10.3402/tellusa.v66.23966>
- Sein, D. V., Mikolajewicz, U., Groger, M., Fast, I., Cabos, W., Joaquim, G. P., Stefan, H., Tido, S., Alfredo, I., & Daniela, J. (2015). Journal of Advances in Modeling Earth Systems. *Journal of Advances in Modeling Earth Systems*, 6, 513–526. <https://doi.org/10.1002/2015MS000470>.Received
- Silva, J. R. de A., Ramos, A. de S., Machado, M., de Moura, D. F., Neto, Z., Canto-Cavalheiro, M. M., Figueiredo, P., do Rosário, V. E., Amaral, A. C. F., & Lopes, D. (2011). A review of antimalarial plants used in traditional medicine in communities in Portuguese-Speaking countries: Brazil, Mozambique, Cape Verde, Guinea-Bissau, São Tomé and Príncipe and Angola. *Memorias Do Instituto Oswaldo Cruz*, 106(SUPPL. 1), 142–158. <https://doi.org/10.1590/S0074-02762011000900019>
- Stagge, J. H., Tallaksen, L. M., Gudmundsson, L., Van Loon, A. F., & Stahl, K. (2015). Candidate Distributions for Climatological Drought Indices (SPI and SPEI). *International Journal of Climatology*, 35(13), 4027–4040. <https://doi.org/10.1002/joc.4267>
- Sultan, B., & Gaetani, M. (2016). Agriculture in West Africa in the twenty-first century: Climate change and impacts scenarios, and potential for adaptation. *Frontiers in Plant Science*, 7(AUG2016), 1–20. <https://doi.org/10.3389/fpls.2016.01262>
- Sylla, B. M., Diallo, I., & S., J. (2013). West African Monsoon in State-of-the-Science Regional Climate Models. *Climate Variability - Regional and Thematic Patterns*, May 2014, 2–36. <https://doi.org/10.5772/55140>
- Valcke, S. (2013). The OASIS3 coupler: a European climate modelling community software. *Geoscientific Model Development*, 6(2), 373–388. <https://doi.org/10.5194/gmd-6-373-2013>
- van Ulden, A. P., & van Oldenborgh, G. J. (2006). Large-scale atmospheric circulation biases and changes in global climate model simulations and their importance for climate change in Central Europe. *Atmospheric Chemistry and Physics*, 6(4), 863–881. <https://doi.org/10.5194/acp-6-863-2006>
- Vasconcelos, R., Brito, J. C., Carranza, S., & Harris, D. J. (2013). Review of the distribution and conservation status of the terrestrial reptiles of the Cape Verde Islands. *Oryx*, 47(1),

77–87. <https://doi.org/10.1017/S0030605311001438>

- Vondou, D. A., & Haensler, A. (2017). Evaluation of simulations with the regional climate model REMO over Central Africa and the effect of increased spatial resolution. *International Journal of Climatology*, *37*, 741–760. <https://doi.org/10.1002/joc.5035>
- Wang, D., Liu, Q., Huang, R. X., Du, Y., & Qu, T. (2006). Interannual variability of the South China Sea throughflow inferred from wind data and an ocean data assimilation product. *Geophysical Research Letters*, *33*(14), 40–43. <https://doi.org/10.1029/2006GL026316>
- Wang, J., & Kotamarthi, V. R. (2015). High-resolution dynamically downscaled projections of precipitation in the mid and late 21st century over North America. *Earth's Future*, *3*(7), 268–288. <https://doi.org/10.1002/2015EF000304>
- Weber, T., Cabos, W., Sein, D. V., & Jacob, D. (2022). Benefits of simulating precipitation characteristics over Africa with a regionally-coupled atmosphere–ocean model. *Climate Dynamics*, *60*(3–4), 1079–1102. <https://doi.org/10.1007/s00382-022-06329-7>
- World Bank-GFDRR. (2020). *Cabo Verde emergency preparedness and response diagnostic: Building a culture of preparedness*. 1–88. https://www.gfdr.org/sites/default/files/publication/R2R_Diagnostic_Cabo_Verde_Report_28Web%29_0.pdf<https://www.preventionweb.net/publications/view/72936>
- Xu, Z., Han, Y., & Yang, Z. (2019). Dynamical downscaling of regional climate: A review of methods and limitations. *Science China Earth Sciences*, *62*(2), 365–375. <https://doi.org/10.1007/s11430-018-9261-5>
- Zhang, L., Sielmann, F., Fraedrich, K., Zhu, X., & Zhi, X. (2015). Variability of winter extreme precipitation in Southeast China: contributions of SST anomalies. *Climate Dynamics*, *45*(9–10), 2557–2570. <https://doi.org/10.1007/s00382-015-2492-6>
- Zhu, S., Remedio, A. R. C., Sein, D. V., Sielmann, F., Ge, F., Xu, J., Peng, T., Jacob, D., Fraedrich, K., & Zhi, X. (2020). Added value of the regionally coupled model ROM in the East Asian summer monsoon modeling. *Theoretical and Applied Climatology*, *140*(1–2), 375–387. <https://doi.org/10.1007/s00704-020-03093-8>
- Zou, L., Zhou, T., & Peng, D. (2016). Journal of geophysical research. *Nature*, *175*(4449), 238. <https://doi.org/10.1038/175238c0>

Zu, T., Xue, H., Wang, D., Geng, B., Zeng, L., Liu, Q., Chen, J., & He, Y. (2019). Interannual variation of the South China Sea circulation during winter: intensified in the southern basin. *Climate Dynamics*, 52(3–4), 1917–1933. <https://doi.org/10.1007/s00382-018-4230-3>

Data availability

Model forcing data and observational data are freely available⁶⁻⁷ model output data is not publicly accessible.

⁶ <https://esgf-data.dkrz.de/search/cmip5-dkrz/>

⁷ <https://chc.ucsb.edu/data/chirps>

